

Page 1 of 48

1 **Influence of root cortical aerenchyma on the rhizosphere**  
2 **microbiome of field-grown maize**

3

4 Tania Galindo-Castañeda<sup>1</sup>; Claudia Rojas<sup>2,3</sup>; Ulas Karaöz<sup>4</sup>; Eoin L. Brodie<sup>4</sup>;  
5 Kathleen M. Brown<sup>1</sup>; Jonathan P. Lynch<sup>1</sup>.

6

7 <sup>1</sup>Department of Plant Science, The Pennsylvania State University, University Park,  
8 PA. 16802 USA. <sup>2</sup>Universidad de O'Higgins, San Fernando, Chile and <sup>3</sup>Center of  
9 Applied Ecology and Sustainability (CAPES), Santiago, Chile. <sup>4</sup>Ecology  
10 Department, Earth and Environmental Sciences, Lawrence Berkeley National  
11 Laboratory, Berkeley CA 94720, USA. <sup>2</sup>Department of Environmental System  
12 Service, ETH Zurich , 8092 Zurich, Switzerland

13 **Corresponding author:** Jonathan P. Lynch. Email [JPL4@psu.edu](mailto:JPL4@psu.edu)

14 Funding information: Fulbright Colombia, *Becas Caldas* supported T.G.C. This  
15 research received funding from the Howard G. Buffett Foundation and by the U.S.  
16 Department of Agriculture, National Institute of Food and Agriculture, award  
17 number 2014-67013-21572 to J.P.L. and K.M.B. Part of this work was performed  
18 at the Lawrence Berkeley National Laboratory, under Department of Energy  
19 contract No. DE-AC02-05CH11231.

20

Page 2 of 48

21 **ABSTRACT**

22 The root anatomical phenotype root cortical aerenchyma (RCA) decreases the  
23 metabolic cost of soil exploration and improves plant growth under drought and  
24 low soil fertility. RCA may also change the microenvironment of rhizosphere  
25 microorganisms by increasing oxygen availability or by reducing carbon  
26 rhizodeposition. We tested the hypothesis that plants with contrasting expression  
27 of RCA have different rhizosphere prokaryotic communities. Maize inbreds were  
28 grown in two field sites, Limpopo Province, South Africa and Pennsylvania, USA,  
29 and their rhizosphere soil sampled at flowering. High- and low-nitrogen fertilization  
30 was imposed as separate treatments in the experiment in South Africa. The  
31 rhizosphere microbial composition of plants with contrasting RCA was  
32 characterized by metabarcoding of the 16S rRNA genes. Geographic location was  
33 the most important factor related to the composition of rhizosphere microbial  
34 communities. In the site in South Africa, RCA explained greater percent of variance  
35 (9%) in the composition of microbial communities than genotype (7%). Although  
36 other root anatomical and architectural phenotypes were studied as possible  
37 cofactors affecting the microbial composition, RCA was among the best significant  
38 explanatory variables for the South African site although it was neutral in the  
39 Pennsylvania site. High-RCA rhizospheres significantly enriched OTUs of the  
40 families *Burkholderiaceae* (in South Africa) and *Bacillaceae* (in USA), compared  
41 to low-RCA plants, and OTUs of the families *Beijerinckiaceae* and  
42 *Sphingomonadaceae* were enriched at the two nitrogen levels in high RCA plants

Page 3 of 48

43 in South Africa. Our results are consistent with the hypothesis that RCA is an  
44 important factor for rhizosphere microbial communities, especially under  
45 suboptimal nitrogen conditions.

46

47 Key words: root cortical aerenchyma, rhizosphere microbial communities, low-  
48 nitrogen tolerance, root phenotyping, maize.

## 49 **INTRODUCTION**

50 Root-associated microbes alter plant nutrition and plant health, becoming a key  
51 aspect of root biology for the development of sustainable agriculture. Factors such  
52 as soil type, geographic location, agronomic practices, plant taxa, plant age, and  
53 root exudates, are modifiers of rhizosphere microbial communities as  
54 demonstrated by metagenomic analyses (reviews by Compant et al. 2019 and  
55 Philippot et al. 2013). Despite the fact that roots create and structure the niches of  
56 rhizosphere communities, the effects of specific root phenotypes on microbial  
57 communities are less well known. Promising root phenotypes that improve soil  
58 resource acquisition can be targeted by plant breeding programs to produce new  
59 cultivars suited for the challenges of modern agriculture (Lynch 2019). However,  
60 selection for such phenotypes should not compromise beneficial microbial  
61 associations in the rhizosphere in order to meet the requirements of sustainable  
62 crop production. This is especially true for nitrogen, since microbial transformations  
63 play key roles in regulating nitrogen availability in the rhizosphere by means of

Page 4 of 48

64 nitrogen fixation (Dobbelaere et al. 2003), ammonification, nitrification and  
65 denitrification (Hai et al. 2009; Hinsinger et al. 2009; Li et al. 2014; Zhao et al.  
66 2017). Therefore, understanding the effects of promising root phenotypes on  
67 microbial communities under nitrogen limitation is an important element of  
68 breeding crops with reduced requirements for nitrogen fertilizer.

69 Nitrogen fertilization is a primary economic, environmental, and energy cost of  
70 intensive maize production (FAO 2017; Robertson and Vitousek 2009). Only 33%  
71 of the nitrogen applied to cereal crops is recovered as grain, the rest, which  
72 remains as vegetative biomass or is lost to the environment, accounts for  
73 approximately \$15.9 billion annual loss (Raun and Johnson 1999). A complex  
74 microbial network participates in the nitrogen cycle in the rhizosphere (Højberg et  
75 al. 1996; Neumann and Römheld 2012; Van Deynze et al. 2018), with the  
76 predominant processes depending on the microhabitats created by roots, which  
77 we propose, are in large measure determined by the root architecture and  
78 anatomy.

79 One strategy to help ameliorate excessive use of nitrogen fertilizers and the loss  
80 of nitrogen in maize fields is the selection of cultivars with specific root phenes  
81 (phenes are the elements composing a phenotype (York et al. 2013)) that improve  
82 nitrogen capture (Gaudin et al. 2011; Lammerts van Bueren and Struik 2017;  
83 Lynch 2013; Lynch 2015; Lynch 2019). Specifically, increased root cortical  
84 aerenchyma (RCA), the production of air pockets in the cortical tissue, has been  
85 reported as a response of maize to low nitrogen stress (York et al. 2015). In

Page 5 of 48

86 addition, plants with increased RCA had increased grain yield under suboptimal  
87 nitrogen fertilization (Saengwilai et al. 2014). These results are in accord with the  
88 concept that increased RCA reduces the metabolic cost of soil exploration (Lynch,  
89 2015) especially under resource scarcity, by means of reduction of metabolically  
90 active tissue in the root cortex, and indicate that plant breeding programs could  
91 deploy RCA to develop maize cultivars better adapted to low-nitrogen stress  
92 (Lynch 2019).

93 Root anatomical phenotypes may change the conditions of niches inhabited by  
94 rhizosphere microbes. The production of RCA has major impacts on the  
95 rhizosphere by changing oxygen availability and shifting facultative or anaerobic  
96 microbial functions towards aerobic metabolisms in the vicinities of RCA air  
97 pockets (Arth and Frenzel 2000; Li et al. 2008; Risgaard-Petersen and Jensen  
98 1997). Processes like carbon utilization, nitrogen transformation, and metal  
99 accumulation depend on soil oxygen content and redox potential (Neumann and  
100 Römheld, 2012), and may modify microbial communities in the rhizosphere.  
101 Likewise, roots with reduced RCA may restrict oxygen diffusion to the rhizosphere,  
102 thereby limiting aerobic microbial metabolism and nutrient utilization.

103 Previous studies have analyzed the microbial composition of the rhizosphere using  
104 high-throughput amplicon sequencing of soils associated with agriculturally  
105 relevant plants, including maize (Bakker et al. 2015; Dohrmann et al. 2013; Li et  
106 al. 2014; Peiffer et al. 2013, Walters et al. 2018). Root architectural traits sus as  
107 root class and order (reviewed by Saleem, 2018), and specific root length are

Page 6 of 48

108 significant factors explaining microbial community composition of the rhizosphere  
109 (Pérez-Jaramillo et al. 2017). Also, decrease in specialist microbial OTUs were  
110 reported from finer to coarser root classes of two cultivars of field-grown *Nicotiana*  
111 *tabacum* (Saleem et al. 2016). To our knowledge, no high-throughput amplicon  
112 sequencing studies of the rhizosphere have studied RCA and its associations with  
113 rhizosphere microbial communities under nitrogen stress. The study of phenotypic  
114 effects on the rhizosphere microbiome under low nutrient stress is important to  
115 inform plant-breeding programs targeting root phenes and better root microbiomes  
116 in the context of sustainable agriculture. This study addressed the effects of RCA  
117 on the composition of rhizosphere bacterial and archeal communities (prokaryotes,  
118 referred as microbial communities here on) of maize under field conditions,  
119 focusing on the comparison of specific OTUs between plants with contrasting  
120 levels of RCA under optimal and suboptimal nitrogen fertilization. Using  
121 metabarcoding of 16S rRNA genes of total rhizosphere DNA, combined with root  
122 phenotyping in two experimental maize fields, we tested the hypothesis that RCA  
123 has significant effects on the microbial community composition.

124

## 125 **MATERIALS AND METHODS**

### 126 **Field experiment and sampling**

127 ***Experimental conditions and plant material.*** Two experiments were conducted,  
128 one at the Russell E. Larson Research and Education Center of the Pennsylvania

Page 7 of 48

129 State University in Rocksprings, PA, USA (designated herein as **RS**) (40°42'37".52  
130 N, 77°57'07".54 W, 366 masl), from June – August 2012; the other at The Ukulima  
131 Root Biology Research Center (designated herein as **URBC**), Limpopo province,  
132 Republic of South Africa (24°33'00.12 S, 28°07'25.84 E, 1235 masl) from  
133 December 2013 to February 2014. Recombinant inbred maize lines (RILs) differing  
134 in RCA formation from the IBM population (B73 x Mo17) (URBC High-RCA:  
135 IBM031, IBM196; URBC Low-RCA: IBM001, IBM345; RS High-RCA: IBM031,  
136 IBM034, IBM177, RS-Low-RCA: IBM001, IBM157, IBM338) (Kaeppler et al. 2000;  
137 Senior et al. 1996) were planted in three row-plots with 0.76 m inter-row spacing  
138 and 0.23 m in-row spacing for a final population of 57,278 plants\*ha<sup>-1</sup>. The soil at  
139 the experimental sites consisted of a Hagerstown silt loam (fine, mixed, semiactive,  
140 mesic Typic Hapludalf) at RS and a clovelly loamy sand (Typic Ustipsamment) at  
141 URBC. Soil test reports from the two sites are summarized in Supplementary Table  
142 1. Contrasting levels of nitrogen fertilization were imposed at URBC according to  
143 soil analyses at the beginning of the field season in order to provide low nitrogen  
144 (33 kg\*ha<sup>-1</sup> applied at URBC) treatment to half of the blocks and high nitrogen  
145 conditions (fertilized with 207 kg\*ha<sup>-1</sup> at URBC, and 150 kg\*ha<sup>-1</sup> at RS) to the other  
146 half. At RS, each block was a 0.4 ha separate field and at URBC the blocks were  
147 randomly distributed in a 20-ha irrigation pivot. In both locations, all nutrients  
148 except nitrogen were adjusted to meet the requirements for maize production as  
149 determined by soil tests. Pest control and irrigation were carried out as needed.  
150 The RS experiment was a complete randomized block design and the URBC

Page 8 of 48

151 experiment was a completely randomized design with genotypes as treatments.  
152 The experiment at RS had three replicates, and the experiment at URBC had four  
153 replicates; all replicates were designated as blocks.

154 ***Rhizosphere and bulk soil sampling.*** Two plants per genotype were excavated  
155 from the central row at flowering (12 weeks after planting at RS and 13 weeks after  
156 planting at URBC) with a shovel inserted approximately 40 cm radial distance from  
157 the stem, and 30 cm depth. The root systems were processed similar to Lundberg  
158 et al. (2012) with modifications in order to scale the method to maize and field  
159 studies. Briefly, the root crowns were excavated, kept in paper bags and  
160 immediately transported to the sample processing station, adjacent to the field.  
161 The root crowns were carefully shaken and ten nodal roots (two to three root  
162 segments per whorl, from the second to the fifth whorl) per plant were aseptically  
163 clipped and placed into 250 mL sterile plastic bags. A total of 20 root fragments  
164 (~40 g fresh weight) per plot were collected. The samples were kept at 4°C for  
165 maximum 24 h, and the rhizosphere samples collected in 150 mL of a 20% sterile  
166 Tween®20 solution (Amresco, Inc., Solon, OH, USA) poured into the plastic bag.  
167 Each closed plastic bag containing roots, soil and tween solution was manually  
168 shaken for 1 min. Then, the solution with the released soil was filtered with nylon  
169 cell strainers (MACS® SmartStrainers, 100 µm), and the filtrate centrifuged at  
170 3,000 g for 15 min. The soil pellet was immediately processed for DNA extraction  
171 for RS, and stored at -20°C for 24 h and then placed at -70°C for URBC. For the  
172 URBC samples, the frozen soil pellet was lyophilized (Labconco System Freezone,



Page 9 of 48

173 1L freeze-drier coupled to a 117 L\*min<sup>-1</sup> vacuum pump) for 48 h to constant weight.  
174 Three samples of bulk soil were taken per plot using a corer of 5.1 cm diameter  
175 inserted 20 cm depth in locations free of plant roots in the furrow, pooled (all the  
176 samples coming from the different genotypes were collected in the same field  
177 replicate), and ~ 10 g diluted in tween solution and filtered through nylon cell  
178 strainers and the filtrate processed as described for rhizosphere samples. The  
179 lyophilized soil samples were aseptically stored in 2 ml vials at 4°C for 2 weeks  
180 and transported to the USA for DNA processing.

181 ***Sampling for root phenotyping.*** Three root crowns per plot were excavated and  
182 sampled for anatomical analysis as previously described (York et al. 2015). These  
183 plants were different to the plants used for DNA extraction with the purpose of  
184 avoiding changes in root anatomy due to the DNA extraction processing on the  
185 roots used for rhizosphere soil collection. Root anatomy was measured on root  
186 cross-sections with the software *RootScan* (Burton et al. 2012). At URBC, two of  
187 the three plants selected for anatomical sampling were also used for architecture  
188 phenotyping with “DIRT” (Bucksch et al., 2014). Washed root crowns were imaged  
189 on a table with black background using a Nikon D70s digital camera with focal  
190 length ranging 22 – 29 mm, exposure time of 1/30 – 1/50 sec., maximal aperture  
191 of 3.6 – 4.1, and digital zoom only. The camera was mounted on a tripod at 50 cm  
192 above the imaging board. All the images were taken at a resolution of 3,008 x  
193 2,000 pixels. For RCA, individual values were assigned to qualitative ranks (high,  
194 intermediate and low) based on values of percentage of cortical area that is

Page 10 of 48

195 aerenchyma in order to facilitate some statistical analysis (PERMANOVAS to  
196 compare genotype vs. phenotype effect, and to plot PCoAs by RCA levels) as  
197 described below (see Fig. 4).

#### 198 **DNA extraction**

199 Soil samples weighing 0.25 g of either of centrifuged rhizosphere (at RS) or  
200 lyophilized soil (at URBC) were processed with the PowerLyzer Power Soil DNA  
201 Kit extraction (MoBio Laboratories, Inc., Carlsbad, CA). Concentration and quality  
202 (260/280 and 230/260 absorbance ratios) were measured with a NanoDrop 1000  
203 Spectrophotometer (Thermo Fisher Scientific Inc.). Integrity of the extracted DNA  
204 was confirmed (> 10 kb) in 0.8% agarose electrophoresis gels (110V for 1.5 h) by  
205 comparison of the extracted DNA stained with ethidium bromide with a molecular  
206 weight marker (2-Log DNA ladder, New England Biolabs® Inc.). The DNA samples  
207 were stored at -70 °C (18 months for RS and a week for URBC). Double-stranded  
208 DNA concentration was measured by fluorescence with a SPECTRAMax GEMINI-  
209 XPS microplate reader (Molecular devices, Sunnyvale, CA, USA) and with  
210 picogreen nucleic acid stain.

#### 211 **16S rRNA amplification and sequencing**

212 DNA concentrations were normalized to 1 – 5 ng  $\mu\text{l}^{-1}$ , and used for triplicate PCRs  
213 with the 515F-806R primer pair, targeting archaeal and bacterial 16S rRNA,  
214 including barcodes as previously described (Caporaso et al. 2012). PCR  
215 conditions and product purification were as follows: one denaturation cycle at 94°C

Page 11 of 48

216 for 3 min followed by 30 annealing cycles (95°C for 30 sec, 52°C for 45 sec, and  
217 72°C for 90 sec); and an extension cycle at 72°C for 12 min, and hold at 4°C in a  
218 MyCycler thermal cycler (Bio-Rad, Hercules, CA, USA). PCR products of the three  
219 reactions were pooled into a single sample, purified with 0.1% carboxyl-modified  
220 Sera-Mag Magnetic Speed-beads™ (Fisher), and eluted in 1x TE for  
221 quantification. Concentrations of the purified PCR products of individual samples  
222 were determined by fluorescence with a SPECTRAMax GEMINI-XPS microplate  
223 reader (Molecular devices, Sunnyvale, CA, USA). The quality was assessed via a  
224 2100 Bionalyzer (Agilent Technologies, Wilmington, USA). The samples were then  
225 pooled into a 25 ng\* $\mu\text{L}^{-1}$  (57.7 nM) library. Number of Illumina-amplifiable DNA  
226 fragments in the library were 2nM, determined by qPCR with the KAPA kit  
227 (Biosystems. Boston, MA, USA) and confirmed with a 2-point Qubit 2.0 fluorometer  
228 (Invitrogen). The library was denatured with 10  $\mu\text{L}$  of 0.2N NaOH and diluted in a  
229 solution of denatured PhiX, for a final library concentration of 10 pM. Sequencing  
230 of the amplicons were performed in an Illumina MiSeq system (Illumina, San  
231 Diego, CA, USA) with 500 cycles.

### 232 **Sequence analysis**

233 The Illumina sequence data was demultiplexed, quality filters applied,  
234 dereplicated, and OTUs (Operational Taxonomic Units) assigned as previously  
235 described with the pipeline UPARSE with default options: Quality score of 16, OTU  
236 radius of 3%, and no length trimming (Edgar 2013). We used 97% similarity cutoff  
237 to assign biological identities to the OTUs by comparison against the database

Page 12 of 48

238 SILVA (Quast et al. 2013). Non-classified OTUs at the domain levels (Bacteria or  
239 Archaea), chimera and singleton sequences were discarded with Qiime (Caporaso  
240 et al. 2010). Dataset preparation for downstream analysis including the taxonomy,  
241 OTU count table, phylogenetic tree and sample information was performed with  
242 the R package Phyloseq (McMurdie and Holmes 2013; R Core Team, 2020).

### 243 **Data analysis**

244 **OTU preprocessing.** The obtained OTUs were analyzed separately by  
245 experiment. Low-count OTUs detected less than more than 2 times in fewer than  
246 at least 10% of the samples were eliminated from the OTU table of each  
247 experiment. **Species diversity.** For diversity calculations one of the URBC  
248 samples with relatively low read-count (less than 10% of the second lowest read-  
249 count) and one sample with low OTUs (236 compared to 1115 OTUs in the second  
250 lowest OTU counts) at RS were dropped for further analyses. Alpha diversity  
251 analyses with the Shannon diversity index were performed on observed OTU  
252 counts. OTU tables were randomly subsampled without replacement (rarefied to  
253 the minimum number of OTUs for the samples of each experiments, 21268 for  
254 URBC and 22358 for RS) in order to perform beta diversity analyses. To study the  
255 beta diversity among samples, meaning the difference of shared microbial OTUs  
256 per taxa among different samples, we used UniFrac distance metrics, which  
257 measures the relatedness of samples based on phylogenetic distance of their taxa  
258 (Lozupone et al. 2010). Unweighted UniFrac distance takes into account the  
259 composition of each sample, while the weighted UniFrac accounts for the

Page 13 of 48

260 abundance of each taxa. Weighted and unweighted UniFrac distances on the  
261 rarefied OTU tables were used to perform principal coordinate analysis (PCoA),  
262 permutational multivariate analyses of variance (PERMANOVA), and constrained  
263 correspondence analyses (CCA). PCoA was used to observe patterns in sample  
264 aggregation by nitrogen levels at URBC, and by genotypes, rhizosphere versus  
265 bulk soil, and significant root phenotypes at the two sites. PERMANOVAS revealed  
266 the effect of nitrogen, genotype and RCA (transformed to qualitative ranges) on  
267 the microbial communities, and CCA was used to measure the variation in  
268 rhizosphere microbial communities explained by specific root phenes measured  
269 as a mean to understand the relative contribution of RCA in comparison with other  
270 root phenes. For CCA analysis we used quantitative values resulting from  
271 phenotyping. Due to the high number of phenotypic variables resulting from  
272 *RootScan* and DIRT, prior to the CCA, we performed a selection of the most  
273 significant variables with random permutations using the function `ordistep` of the R  
274 package *Vegan* (Oksanen et al. 2017). The resulting variables were then included  
275 in the model of the ordination. The significance of the model and of the phenes  
276 included in the model were calculated with permutation tests with the function  
277 `anova.cca` of the R package *Vegan*. **Phenotype-sensitive OTUs**. Association of  
278 significantly enriched OTUs with contrasting root phenotypes were performed by  
279 fitting a generalized linear model with a negative binomial distribution to normalized  
280 abundance values. We used the “trimmed means of M” method for the  
281 normalization available through the BioConductor package *edgeR* (McCarthy et al.

Page 14 of 48

282 2012; Robinson et al. 2010) and expressed the normalized counts as relative  
283 abundance counts per millions (CPM) for each OTU in each site and nitrogen level.  
284 To test for differential abundance, we used a likelihood ratio tests (LRT) with the  
285 R package edgeR. OTUs that were significantly increased or depleted (compared  
286 to the control treatment by a significantly different fold-factor, see results section  
287 for more details on the specific control treatment used for each comparison) with  
288  $P$  values  $< 0.01$ , were considered phenotype-responsive. **Plant phenotyping.** The  
289 effect of root architectural and anatomical phenotypes (with special focus on  
290 RCA) on UniFrac distance metrics was assessed with the scale-transformed  
291 quantitative values of the measured phenotypes retrieved by *RootScan* and DIRT.  
292 RCA was grouped into categorical states and assigned to each root sample for the  
293 PCoA.  
294

## 295 **RESULTS**

### 296 **Taxonomy and diversity**

297 A total of 3,403,932 high quality sequences were obtained from the two  
298 experimental sites with a median read count per sample of 59,718 (range of 1,865  
299 – 126,242). 17,693 microbial OTUs resulted from the alignment of the sequences  
300 with the SILVA dataset (Quast et al. 2013). After low-count OTU removal, the total  
301 sequences decreased from 951,299 to 941,051 at RS, and from 2,452,633 to  
302 2,394,705 at URBC; and the total number of OTUs from 12,478 to 6,125 at RS and  
303 from 14,073 to 5,536 at URBC.

304 There were 34 and 45 phyla found at URBC and RS respectively. *Proteobacteria*,  
305 *Acidobacteria*, *Actinobacteria*, *Verrucomicrobia*, *Bacteroidetes*, and *Firmicutes*  
306 were among the most abundant phyla overall (Fig. 1). Rhizosphere soil at the two  
307 sites had a greater proportion of *Proteobacteria* and *Bacteroidetes*, and smaller  
308 proportion of *Acidobacteria* and *Nitrospirae* than bulk soil. *Gemmatimonadetes*,  
309 *Chloroflexi* and *Thaumarchaeota* were reduced in the rhizosphere at URBC but  
310 not at RS. Eleven phyla were unique to RS (for example, *Hydrogenedentes*,  
311 *Zixibacteria*, *Nitrospinae*, *Atribacteria*) while all the phyla found in URBC were also  
312 present in RS. *Sphingomonadaceae* and *Burkholderiaceae* (both from Phylum  
313 *Proteobacteria*) and *Micrococcaceae* (phylum *Actinobacteria*) were the most  
314 abundant families at URBC (Supplementary Fig. 1a). *Sphingobacteriaceae*,  
315 *Beijerinckiaceae*, and *Rhodanobacteraceae* were among the most abundant  
316 families at URBC but not among the most abundant families at RS.

Page 16 of 48

317 *Sphingomonadaceae*, *Burkholderiaceae*, and *Xanthobacteraceae* (Phylum  
318 *Proteobacteria*) were the most abundant families at RS (Supplementary Fig. 1b).  
319 RS had greater OTU richness compared to URBC, and bulk soil had greater  
320 average species diversity than rhizosphere soil at URBC (Fig. 2).

### 321 **Nitrogen, genotype, RCA and rhizosphere effect on microbial communities**

322 Microbial communities separated mainly by site (PCoA 1, Fig. 3) although there  
323 was a remarkable overlap of the community structure of bulk soil at URBC with  
324 bulk and rhizosphere soil communities at RS. Bulk soil samples ordinated apart  
325 from rhizosphere regardless of the nitrogen level at URBC (Supplementary Fig. 2).  
326 Genotype was not a significant grouping factor at either of the two locations (Fig.  
327 3, Supplementary Fig. 2, Table 1). Transformed RCA values into qualitative ranks  
328 (Supplementary Table 3) had not significant effect on the weighted UniFrac  
329 distance at neither of the two sites (Table 1). RCA explained a greater amount of  
330 variation (9.5%) compared to genotype (7.6%) at URBC but the opposite was  
331 found at RS (Table 1). There was a significant effect of soil type (rhizosphere vs.  
332 bulk soil) at the two sites (Supplementary Table 2) but the percent of variation in  
333 beta diversity explained by soil type was over three times greater at URBC  
334 compared to RS. This stronger rhizosphere effect at URBC can be seen by  
335 comparing weighted-UniFrac distances between RCA phenotypes (separated by  
336 ranks) and bulk soils (Supplementary Fig. 3).

### 337 **Effect of RCA on microbial communities**



Page 17 of 48

338 Contrasting RCA phenotypes were found among the plants evaluated (Fig. 4,  
339 Supplementary Table 3). Ordination plots of UniFrac distances by RCA (ranked  
340 according to Supplementary Table 3 and Fig. 4) show microbial communities of  
341 high and low RCA separated in the first component (Fig. 5). Ranges and other  
342 descriptive statistics of the complete set of anatomical and architectural phenes  
343 measured are provided in Supplementary Table 4 and Supplementary Table 5. All  
344 such phenes were used to select significant models and the resulting models are  
345 presented in Table 2. The effect of specific root phenes on rhizosphere microbial  
346 communities depended on site, and different models were selected with random  
347 permutations (Table 2). The selected models were then used with CCA (controlling  
348 for genotype and block - and nitrogen at URBC) to assess the effect of quantitative  
349 phene values on the unweighted and weighted UniFrac distances. Among the  
350 anatomical and architectural phenes measured at URBC (Table 2), RCA was  
351 significant for the unweighted ( $P=0.045$ , Table 2) and weighted ( $P=0.092$ , Table 2)  
352 UniFrac distances; and BottomAngle was significant ( $P=0.068$ , Table 2) for  
353 unweighted UniFrac distance, while D10 was significant ( $P=0.062$ , Table 2) for the  
354 weighted UniFrac distance. Among the anatomical variables measured at RS no  
355 significant models (with  $P < 0.1$ ) were found for the weighted or the unweighted  
356 UniFrac distances. Diversity of rhizosphere microbial communities was greater in  
357 high RCA compared to low RCA under low nitrogen at URBC (Fig. 6). The effect  
358 of RCA on specific OTUs at the two experimental sites was further investigated.

359 **Phenotype-sensitive OTUs**

Page 18 of 48

360 High-RCA plants had specific sets of rhizosphere prokaryotes that were  
361 significantly enriched or depleted compared to low-RCA plants (Fig. 7,  
362 Supplementary Fig. 4, Supplementary Fig. 5). At URBC, high-RCA rhizospheres  
363 hosted 95 significantly enriched OTUs and had 40 significantly decreased OTUs  
364 compared to low-RCA rhizospheres under high nitrogen. A similar ratio between  
365 enriched (43) and decreased (16) OTUs was found when comparing high and low  
366 RCA under low nitrogen (Fig. 7) at URBC. Also, alpha diversity between plant  
367 phenotypes (Fig. 6) show an increase of number of OTUs associated with high  
368 RCA phenotypes at URBC and low nitrogen, as well as the specific abundance  
369 values of OTUs by phylum and family (Supplementary Fig. 6 and Supplementary  
370 Fig. 7). When compared to bulk soil, rhizospheres of high-RCA plants had also a  
371 greater number of significantly enriched OTUs than low-RCA rhizospheres  
372 (Supplementary Fig. 4a), as well as a greater number of unique significantly  
373 enriched and decreased OTUs (Supplementary Fig. 4b). RCA phenotype had a  
374 weaker effect on the rhizosphere communities under high nitrogen at RS as there  
375 were fewer significantly enriched and depleted OTUs associated to each RCA  
376 phenotype (Fig. 7). The weaker rhizosphere effect at RS is also evident when the  
377 microbial communities of contrasting RCA phenotypes were compared to bulk soil  
378 (Supplementary Fig. 3 and Supplementary Fig. 5).

379 At URBC, RCA-sensitive OTUs from high RCA phenotypes shared some common  
380 features between high and low nitrogen. Significantly enriched microorganisms in  
381 high-RCA under high nitrogen (as shown in Fig. 7) belonged mainly to the phyla

Page 19 of 48

382 *Proteobacteria* (29.9% of the total enriched OTUs), *Acidobacteria* (27%),  
383 *Actinobacteria* (11.34%), *Bacteroidetes* (11.34%), and *Thaumarchaeota* (11.34%)  
384 and in minor proportions to the phyla *Chloroflexi* and *Firmicutes* (Supplementary  
385 Fig. 6a), similar to the distribution of the enriched OTUs in high-RCA rhizospheres  
386 of low nitrogen plots with *Proteobacteria* (34%), *Chloroflexi* (20%), *Bacteroidetes*  
387 (16%), and *Acidobacteria* (14%) and smaller proportions of *Actinobacteria* and  
388 *Firmicutes* (Supplementary Fig. 6b, Supplementary File S1). At the family level,  
389 High-RCA plants of the two nitrogen levels at URBC had some families  
390 significantly-enriched in common (although OTUs did not overlap) such as  
391 *Beijerinckiaceae*, *Burkholderiaceae*, *Haliangiaceae*, *Longimicrobiaceae*,  
392 *Microscillaceae*, *Chitinophagaceae*, *Bacillaceae*, *Paenibacillaceae*,  
393 *Polyangiaceae*, *Solibacteraceae*, and *Thermoanaerobaculaceae* (Supplementary  
394 Fig. 7).

395 There was greater diversity among the enriched OTUs of high-RCA plants at high  
396 nitrogen compared to low nitrogen at URBC. Enriched OTUs from the phyla  
397 *Thaumarchaeota*, *Gemmatimonadetes*, *Planctomycetes*, and *Dependentiae* in  
398 high-RCA plants were associated with high nitrogen, while an enrichment of OTUs  
399 from the phyla *Armatimonadetes* and *Cyanobacteria* were associated with low  
400 nitrogen (Supplementary Fig. 6). Several families were unique to high-RCA plants  
401 at each nitrogen level (Supplementary Fig. 7). Among the OTUs with the greatest  
402 abundance at high-RCA in high nitrogen, the families *Burkholderiaceae*,  
403 *Sphingomonadaceae*, *Nitrososphaeraceae*, had the most abundant significantly

Page 20 of 48

404 enriched OTUs compared to low-RCA rhizospheres (Supplementary Fig. 7). The  
405 most abundant OTUs enriched at low-RCA and high nitrogen belonged to the  
406 families *Burkholderiaceae* and *Chitinophagaceae*, and *Sphingobacteriaceae*. With  
407 low nitrogen and high-RCA, *Burkholderiaceae* had the most abundant OTUs. The  
408 families *Beijerinckiaceae*, *Bacillaceae*, *Burkholderiaceae* and *Chitinophagaceae*  
409 had OTUs that were shared between high and low nitrogen in high RCA plants,  
410 and that were among the most abundant and significantly enriched OTUs  
411 (Supplementary Fig. 7).

412 High-RCA rhizosphere of high-nitrogen plots at RS had 35 enriched OTUs. There  
413 was one shared OTU between URBC and RS that was depleted in high RCA roots  
414 (OTU 11202, an unclassified species of the family *Rhodanobacteraceae* (order  
415 *Xanthomonadales*, phylum Proteobacteria), (Fig. 7b). Enriched OTUs of high-RCA  
416 in RS were distributed among *Planctomycetes* (39% of the total enriched OTUs),  
417 *Acidobacteria* (17%) and *Proteobacteria* and *Actinobacteria* (14%), and in smaller  
418 proportions among *Firmicutes* (8%), and other phyla (<8%) (Supplementary Fig.  
419 8, Supplementary File S1); whereas the 45 enriched OTUs of low-RCA  
420 rhizospheres at RS had a contrasting phyla distribution with *Proteobacteria* (44%),  
421 *Bacteroidetes* (16%) as dominant phyla followed by *Actinobacteria* (13%),  
422 *Planctomycetes* (9%) and *Acidobacteria* (6%) and other phyla (<6%). The most  
423 abundant OTUs in RS belonged to the genus *Oceanobacillus* (family *Bacillaceae*)  
424 in high-RCA plants, and to the genus *Aquicella* (family *Diplorickettsiaceae*) in low-  
425 RCA plants.

426 **DISCUSSION**

427 Contrasting levels of RCA of field-grown maize were associated with specific  
428 compositions of the rhizosphere microbiome and the extent of this association  
429 depended on the geographic location, being more defined at URBC (South Africa).  
430 Regardless of the nitrogen fertilization treatment, RCA was associated with a set  
431 of significantly enriched OTUs under an intensively managed agricultural sandy  
432 soil in South Africa but had no significant effect on the rhizosphere microbial  
433 richness in a finer-textured soil of Pennsylvania (USA). Our results indicate that  
434 root phenotypes may explain part of the variability in the rhizosphere microbial  
435 composition and constitute a starting point to further study root phenotype effects  
436 on the root microbiome of agricultural species.

437 The dominant phyla *Proteobacteria*, *Acidobacteria*, *Bacteroidetes* and  
438 *Actinobacteria* found here overlap those reported among the dominant phyla in  
439 agricultural and rhizosphere soils (Lundberg et al. 2012; Peiffer et al. 2013;  
440 Philippot et al. 2013; Sul et al. 2013). The stronger rhizosphere effect observed at  
441 URBC (South Africa) compared to RS (USA) could be explained by differences in  
442 soil properties and agricultural management of the two sites. The sandy, low  
443 organic matter soil at URBC may have offered a more restrictive environment for  
444 microbial growth compared to the more fertile silt-loam at RS (Supplementary  
445 Table 1). Additionally, crop rotations at RS in comparison with maize after maize  
446 monoculture at URBC could have provided more diverse microbial communities at  
447 RS (Fig. 2). Therefore, root phenotypes had a significant impact on soil

Page 22 of 48

448 microorganisms at URBC (Supplementary Fig. 3, Supplementary Fig. 4), where  
449 soils contain less organic matter (<0.5%, Supplementary Table 1) and are coarser  
450 in texture than RS, leading to less well-developed soil structure. Better soil  
451 structure (e.g. more aggregates) creates more diverse microenvironments and  
452 contributes to greater microbial diversity (Fierer 2017; Sexstone et al. 1985).  
453 Likewise, greater organic matter content can be associated with greater microbial  
454 diversity due to the more diverse carbon sources for microbial decomposition (Sul  
455 et al. 2013). Accordingly, RCA separated the microbial communities at URBC,  
456 where there was a significant rhizosphere effect (Fig. 5, Supplementary Fig. 3, and  
457 Supplementary Table 2), while no separation by RCA levels was observed at RS.  
458 Despite the differences in rhizosphere effects between the two sites, it is  
459 noteworthy to find two enriched (*Proteobacteria* and *Bacteroidetes*) and two  
460 depleted (*Acidobacteria* and *Nitrospirae*) phyla in maize rhizospheres of the two  
461 sites, in accord with previous studies in which *Proteobacteria* and *Bacteroidetes*  
462 were enriched (Bakker et al. 2015; Peiffer et al. 2013) and *Acidobacteria* depleted  
463 in the rhizosphere soil (Fierer et al. 2007; Niu et al. 2017; Peiffer et al. 2013).  
464 Among the significantly depleted or enriched OTUs at contrasting levels of RCA  
465 found here, the genera *Agromyces*, *Bacillus*, *Caulobacter*, *Chthoniobacter*,  
466 *Flavobacterium*, *Nocardioides* and *Sphingomonas* were recently reported as part  
467 of the maize core microbiome (Walters et al. 2018). These findings demonstrate  
468 the intrinsic selectivity of soil microbial communities and the potential importance  
469 of RCA (and possibly other root phenes) on changing the composition of the

Page 23 of 48

470 communities in the rhizosphere. Additionally, and similar to our results, Dohrmann  
471 et al. (2013) found that nitrifiers were slightly enriched in the rhizosphere of  
472 genetically modified Bt field-grown maize but they found bacteria (*Nitrosomonas*  
473 and *Nitrospira*) as opposed to the ammonia oxidizing archaeans of the family  
474 *Nitrososphaeraceae* found here. Dohrmann et al. (2013) suggested that their  
475 enrichment of nitrifying bacteria could be linked to a greater protein content in Bt  
476 maize due to the possible overexpression of Cry proteins. Since ammonia  
477 oxidizing archaeans outcompete ammonia oxidizing bacteria under lower  
478 ammonia concentration (Hatzenpichler 2012), our results at URBC (sandy, low  
479 organic matter content and low pH soil in South Africa) may correspond to  
480 rhizospheres with low nitrogen concentration in high-RCA plants, even under high  
481 nitrogen fertilization. Moreover, enrichment of archaea of the *Nitrososphaeraceae*  
482 family is highly suggestive of changes in nitrification as members of this family are  
483 obligately aerobic chemolithoautotrophs capable of nitrification. They can be  
484 mixotrophic, requiring organic substrates for growth, and this may contribute to  
485 their enrichment in high RCA plants. The mechanisms underlying this merit further  
486 investigation.

487 Our results support the hypothesis that root control of rhizosphere communities  
488 among related genotypes is associated with root phenotypes (Fig. 5, Table 1,  
489 Table 2, Fig. 6). We propose that phenotypes have a stronger, and perhaps more  
490 predictive effect on microbial communities compared to genotype effects as  
491 observed at URBC, with genotypes explaining 7% of variation and RCA explaining

Page 24 of 48

492 9% of the variation (Table 1), this not accounting for other phenes that, in addition  
493 to RCA, might have significant effect on rhizosphere biodiversity. This hypothesis  
494 will need additional support. However, it is noteworthy that genotypic effect of  
495 related maize lines has shown modest or partial effects on rhizosphere microbial  
496 communities in the present and in previous studies (Bakker et al. 2015; Dohrmann  
497 et al. 2013; Fang et al. 2005; Peiffer et al. 2013; Walters et al. 2018), and no  
498 exploration of root phenotypes has been reported to our knowledge in large-scale  
499 microbiome studies of rhizospheres. Moreover, there appear to be root phenes  
500 that are more important than others as drivers of the microbial composition in the  
501 rhizosphere as shown by the CCA analysis - when controlling for nitrogen and  
502 genotype effects (Table 2). The root phenes shaping the rhizosphere communities  
503 varied by site, with RCA significant for the UniFrac distance metrics at URBC.  
504 While the differences in RCA at RS had no significant effects on rhizosphere  
505 microbial diversity, we found a few uniquely enriched taxa with each phenotype  
506 (high and low-RCA) (Fig. 7), with the most abundant taxa (genus *Oceanobacillus*)  
507 being associated with plant growth promotion (Supplementary File S1,  
508 Supplementary results).

509 We propose that the diversity associated with contrasting levels of RCA observed  
510 at URBC may be associated with changes in functions in the rhizosphere microbial  
511 community. More specifically, two possible mechanisms that could be further  
512 studied as factors affecting rhizosphere microbial diversity are the diffusion of  
513 oxygen from aerenchyma lacunae and the rhizodeposition of carbon as influenced



Page 25 of 48

514 by RCA. Greater oxygen concentration and possibly, differences in carbon  
515 rhizodeposition into the rhizosphere of the high-RCA plants may be associated  
516 with the ~2 fold greater number of significantly enriched OTUs observed in high-  
517 RCA plants phenotypes compared to low-RCA plants at URBC under high and low  
518 nitrogen (Fig. 7). Plants with increased RCA may have reduced carbon  
519 rhizodeposition in axial roots as a consequence of the loss of cortical tissue; this  
520 effect may be intensified under low nitrogen given the overall low nitrogen content  
521 of the plant. However, it is also possible that under low nitrogen, plants with  
522 increased RCA have more carbon to invest in rhizodeposition compared to  
523 reduced-RCA plants as an indirect consequence of the benefits of RCA on nitrogen  
524 acquisition under low nitrogen (Saengwilai et al. 2014). Reduced cortical tissue of  
525 high-RCA plants reduces the metabolic burden of soil exploration and nutrient  
526 capture (Lynch 2015).

527 RCA had significant effects on the abundances the ammonia oxidizing archaean  
528 family *Nitrososphaeraceae* in high-RCA plants growing under high nitrogen at  
529 URBC (Supplemental File S1). Enrichment of the archaean *amoA* genes (genes  
530 encoding for the ammonia monooxygenase) were previously found in a study with  
531 field-grown maize rhizosphere (Li et al. 2014) in accordance with our findings. High  
532 abundances of *Nitrososphaeraceae* could cause a net decrease of ammonia in the  
533 rhizosphere, forcing other microbial species or even the plant itself to invest  
534 reductive power in nitrate assimilation or could also promote nitrogen losses from  
535 the rhizosphere if the nitrate generated is lost as leachate or ultimately converted

Page 26 of 48

536 into gaseous nitrogen (Stahl and Torre 2012). The enrichment of  
537 *Nitrososphaeraceae* in high-RCA and high-N plants at URBC could indicate a low  
538 continuous supply of ammonium in accordance with previous research indicating  
539 that archaeal ammonia oxidizers are adapted to lower ammonia availability  
540 (Hatzenpichler 2012; Stahl and Torre 2012; Sterngren et al. 2015). However, since  
541 our analyses are based on taxonomy these hypotheses merit further research.

542 The present study provides insights into the effects of RCA on rhizosphere  
543 microbial communities of maize grown in two contrasting environments, and give  
544 rise to interesting questions and hypotheses for future research. Further research  
545 could be conducted to reveal more detailed effects exploring more root phenotypes  
546 and expanding to root architectural phenes. Here, we found that together with  
547 RCA, rooting angle had significant effects on the communities in the maize  
548 rhizosphere at URBC (Table 2). The use of larger sets of genotypes as well as the  
549 study of the effects of phenotypes in combination with plant developmental stages  
550 will also add to our findings. Additionally, the inclusion of eukaryotes is crucial for  
551 the understanding of the effects of aerenchyma and other phenotypes on the  
552 fungal populations closely related to the root cortex.

553 The selection of plants targeting root ideotypes that improve soil exploration under  
554 low-nutrient and drought stress would be benefited by a concomitant selection of  
555 beneficial microbiomes. This study is a pioneer in this endeavor by suggesting  
556 possible habitat changes provided by contrasting RCA and the associated  
557 microorganisms. Plant and microbiome breeding together could produce ideal

Page 27 of 48

558 combinations of roots and microbes adapted to resource scarcity to improve plant  
559 growth and productivity.

## 560 **ACKNOWLEDGEMENTS**

561 Robert Snyder, Michael Williams, Gustavo da Silveira, Andrew Evensen, Melda  
562 Manchidi Shaku, Tsitso Zechariah Mokoena, Vincent Nkhumeleni Rambau, Javier  
563 Ceja Navarro, and Shi Wang provided technical assistance.  
564 The NVIDIA Corporation donated the Tesla K40 GPU used for this research. We  
565 thank Drs. Mary Ann Bruns and Alexander Bucksch for their discussion and  
566 comments.

## 567 **LITERATURE CITED**

568 Arth, I. Frenzel, P. 2000. Nitrification and denitrification in the rhizosphere of rice:  
569 the detection of processes by a new multi-channel electrode. *Biol. Fertility. Soils*  
570 31:427-435.

571 Bakker, M.G., Chaparro J.M., Manter, D.K., Vivanco, J.M. 2015. Impacts of bulk  
572 soil microbial community structure on rhizosphere microbiomes of *Zea mays*. *Plant*  
573 *Soil* 392:115-126.

574 Bucksch, A., Burrige, J., York, L.M., Das, A., Nord, E., Weitz, J.S., Lynch, J.P.  
575 2014. Image-based high-throughput field phenotyping of crop roots. *Plant Physiol.*  
576 166:470-486.

Page 28 of 48

- 577 Burton, A.L., Williams, M., Lynch, J.P., Brown, K.M. 2012. RootScan: Software for  
578 high-throughput analysis of root anatomical traits. *Plant Soil* 357:189-203.
- 579 Compant, S., Samad, A., Faist, H., and Sessitsch, A. 2019. A review on the plant  
580 microbiome: Ecology, functions, and emerging trends in microbial application. *J.*  
581 *Adv. Res.* 19:29–37.
- 582 Caporaso, J.G., Kuczynski, J., Stombaugh, J., Bittinger, K., Bushman, F.D.,  
583 Costello, E.K., Fierer, N., Peña, A.G., Goodrich, J.K., Gordon, J.I., Huttley, G.A.,  
584 Kelley, S.T., Knights, D., Koenig, J.E., Ley, R.E., Lozupone, C.A., McDonald, D.,  
585 Muegge, B.D., Pirrung, M., Reeder, J., Sevinsky, J.R., Turnbaugh, P.J., Walters,  
586 W.A., Widmann, J., Yatsunenko, T., Zaneveld, J., Knight, R. 2010. QIIME allows  
587 analysis of high-throughput community sequencing data. *Nat. Methods* 7:335.
- 588 Caporaso, J.G., Lauber, C.L., Walters, W.A., Berg-Lyons, D., Huntley, J., Fierer,  
589 N., Owens, S.M., Betley, J., Fraser, L., Bauer, M., Gormley, N., Gilbert, J.A., Smith,  
590 G., Knight, R. 2012. Ultra-high-throughput microbial community analysis on the  
591 Illumina HiSeq and MiSeq platforms. *ISME J* 6:1621.
- 592 Dobbelaere, S., Vanderleyden, J., Okon, Y. 2003. Plant growth-promoting effects  
593 of diazotrophs in the rhizosphere. *Crit Rev Plant Sci* 22:107-149.
- 594 Dohrmann, A.B., Küting, M., Jünemann, S., Jaenicke, S., Schlüter, A., Tebbe, C.C.  
595 2013. Importance of rare taxa for bacterial diversity in the rhizosphere of Bt- and  
596 conventional maize varieties. *ISME J* 7:37-49.

Page 29 of 48

- 597 Edgar, R.C. 2013. UPARSE: highly accurate OTU sequences from microbial  
598 amplicon reads. *Nat. Methods* 10:996-998.
- 599 Fang, M., Kremer, R.J., Motavalli, P.P., Davis, G. 2005. Bacterial diversity in  
600 rhizospheres of nontransgenic and transgenic corn. *Appl. Environ. Microbiol.* 71:  
601 4132-4136.
- 602 FAO. 2017. World fertilizer trends and outlook to 2020. Food and Agriculture  
603 Organization of the United Nations. <http://www.fao.org/3/a-i6895e.pdf>
- 604 Fierer, N. 2017. Embracing the unknown: disentangling the complexities of the soil  
605 microbiome. *Nat. Rev. Microbiol.* 15:579
- 606 Fierer, N., Bradford, M.A., Jackson, R.B. 2007. Toward an ecological classification  
607 of soil bacteria. *Ecology* 88:1354-1364.
- 608 Gaudin, A.C.M., McClymont, S.A., Holmes, B.M., Lyons, E., Raizada, M.N. 2011.  
609 Novel temporal, fine-scale and growth variation phenotypes in roots of adult-stage  
610 maize (*Zea mays* L.) in response to low nitrogen stress. *Plant Cell Environ.*  
611 34:2122-2137.
- 612 Hai, B., Diallo, N.H., Sall, S., Haesler, F., Schauss, K., Bonzi, M., Assigbetse, K.,  
613 Chotte, J-L., Munch, J.C., Schloter, M. 2009. Quantification of key genes steering  
614 the microbial nitrogen cycle in the rhizosphere of sorghum cultivars in tropical  
615 agroecosystems. *Appl. Environ. Microbiol.* 75:4993-5000.

Page 30 of 48

- 616 Hatzenpichler, R. 2012. Diversity, physiology, and niche differentiation of  
617 ammonia-oxidizing archaea. *Appl. Environ. Microbiol.* 78:7501-7510
- 618 Hinsinger, P., Bengough, A.G., Vetterlein, D., Young, I.M. 2009. Rhizosphere:  
619 biophysics, biogeochemistry and ecological relevance. *Plant Soil* 321:117-152.
- 620 Højberg, O., Binnerup, S.J., Sørensen, J. 1996. Potential rates of ammonium  
621 oxidation, nitrite oxidation, nitrate reduction and denitrification in the young barley  
622 rhizosphere. *Soil Biol. Biochem.* 28:47-54
- 623 Kaeppler, S.M., Parke, J.L., Mueller, S.M., Senior, L., Stuber, C., Tracy, W.F. 2000.  
624 Variation among maize inbred lines and detection of quantitative trait loci for  
625 growth at low phosphorus and responsiveness to arbuscular mycorrhizal fungi.  
626 *Crop Sci.* 40:358-364.
- 627 Lammerts Van Bueren, E.T., Struik, P.C. 2017. Diverse concepts of breeding for  
628 nitrogen use efficiency. A review. *Agron Sustain Dev* 37:50.
- 629 Li, X., Rui, J., Xiong, J., Li, J., He, Z., Zhou, J., Yannarell, A.C., Mackie, R.I. 2014.  
630 Functional potential of soil microbial communities in the maize rhizosphere. *PLoS*  
631 *ONE* 9:e112609.
- 632 Li, Y.L., Fan, X.R., Shen, Q.R. 2008. The relationship between rhizosphere  
633 nitrification and nitrogen-use efficiency in rice plants. *Plant Cell Environ.* 31:73-85.
- 634 Lozupone, C., Lladser, M.E., Knights, D., Stombaugh, J., Knight, R. 2010. UniFrac:  
635 an effective distance metric for microbial community comparison. *ISME J* 5:169.

Page 31 of 48

- 636 Lundberg, D.S., Lebeis, S.L., Paredes, S.H., Yourstone, S., Gehring, J., Malfatti,  
637 S., Tremblay, J., Engelbrektson, A., Kunin, V., Rio, T.G.D., Edgar, R.C., Eickhorst,  
638 T., Ley, R.E., Hugenholtz, P., Tringe, S.G., Dangl, J.L. 2012. Defining the core  
639 *Arabidopsis thaliana* root microbiome. *Nature* 488: 86-90
- 640 Lynch, J.P. 2013. Steep, cheap and deep: an ideotype to optimize water and N  
641 acquisition by maize root systems. *Ann. Bot.* 112:347-357.
- 642 Lynch, J.P. 2015. Root phenes that reduce the metabolic costs of soil exploration:  
643 opportunities for 21st century agriculture. *Plant Cell Environ.* 38:1775-1784.
- 644 Lynch, J.P. 2019. Root phenotypes for improved nutrient capture : an  
645 underexploited opportunity for global agriculture. *New Phytol.* doi:  
646 10.1111/nph.15738Lynch, J.P., Wojciechowski, T. 2015. Opportunities and  
647 challenges in the subsoil: pathways to deeper rooted crops. *J. Exp. Bot.* 66:2199–  
648 2210.
- 649 Mccarthy, D.J., Chen, Y., Smyth, G.K. 2012. Differential expression analysis of  
650 multifactor RNA-Seq experiments with respect to biological variation. *Nucleic  
651 Acids Res.* 40: 4288-4297.
- 652 McMurdie, P.J., Holmes, S. 2013. Phyloseq: An R package for reproducible  
653 interactive analysis and graphics of microbiome census data. *PLoS ONE.*  
654 8:e61217.

Page 32 of 48

- 655 Neumann, G., Römheld, V. 2012. Chapter 14 - Rhizosphere chemistry in relation  
656 to plant nutrition. Pages 347-368 in: Marschner's Mineral Nutrition of Higher Plants.  
657 Marschner, P. Ed. San Diego: Academic Press.
- 658 Niu, B., Paulson, J.N., Zheng, X., Kolter, R. 2017. Simplified and representative  
659 bacterial community of maize roots. Proc. Natl. Acad. Sci. USA 114:E2450-E2459.
- 660 Oksanen, J., Blanchet, F.G., Friendly, M., Kindt, R., Legendre, P., Mcglinn, D.,  
661 Minchin, P.R., O'hara, R.B., Simpson, G.R., Solymos, P., Stevens, M.H.H.,  
662 Szoecs, E., Wagner, H. 2017. Vegan: Community ecology package. R package  
663 version 2.4-5.
- 664 Peiffer, J.A., Spor, A., Koren, O., Jin, Z., Tringe, S.G., Dangl, J.L., Buckler, E.S.,  
665 Ley, R.E. (2013) Diversity and heritability of the maize rhizosphere microbiome  
666 under field conditions. Proc. Natl. Acad. Sci. USA 101:6548-6553.
- 667 Pérez-Jaramillo, J.E., Carrión, V.J., Bosse, M., Ferrão, L.F.V., De Hollander, M.,  
668 Garcia, A.F., Ramírez, C.A., Mendes, R., Raaijmakers, J.M. 2017. Linking  
669 rhizosphere microbiome composition of wild and domesticated *Phaseolus vulgaris*  
670 to genotypic and root phenotypic traits. ISME J 11: 2244-2257.
- 671 Philippot, L., Raaijmakers, J.M., Lemanceau, P., Van Der Putten, W.H. 2013.  
672 Going back to the roots: the microbial ecology of the rhizosphere. Nat. Rev.  
673 Microbiol. 11: 789-799.



Page 33 of 48

- 674 Quast, C., Pruesse, E., Yilmaz, P., Gerken, J., Schweer, T., Yarza, P., Peplies, J.,  
675 Glöckner, F.O. 2013. The SILVA ribosomal RNA gene database project: improved  
676 data processing and web-based tools. *Nucleic Acids Res.*41:D590-D596.
- 677 R Core Team (2020) R: A language and environment for statistical computing.  
678 Vienna, Austria. <https://www.r-project.org/>
- 679 Raun, W.R., Johnson, G.V. 1999. Improving nitrogen use efficiency for cereal  
680 production. *Agron J* 91:357-363.
- 681 Risgaard-Petersen, N., Jensen, K. 1997. Nitrification and denitrification in the  
682 rhizosphere of the aquatic macrophyte *Lobelia dortmanna* L. *Limnol. Oceanogr.*  
683 42:529-537.
- 684 Robertson, G.P., Vitousek, P.M. 2009. Nitrogen in agriculture: balancing the cost  
685 of an essential resource. *Annu Rev Environ Resour* 34: 97-125.
- 686 Robinson, M.D., McCarthy, D.J., Smyth, G.K. 2010. edgeR: a Bioconductor  
687 package for differential expression analysis of digital gene expression data.  
688 *Bioinformatics* 26:139-140.
- 689 Saleem, M., Law, A.D., Moe, L.A. 2016. *Nicotiana* roots recruit rare rhizosphere  
690 taxa as major root-inhabiting microbes. *Microb. Ecol.* 71:469-472.
- 691 Saleem, M., Law, A.D., Sahib, M.R., Pervaiz, Z.H., Zhang, Q. 2018. Impact of root  
692 system architecture on rhizosphere and root microbiome. *Rhizosphere* 6:47-51

Page 34 of 48

- 693 Saengwilai, P., Nord, E.A., Chimungu, J.G., Brown, K.M., Lynch, J.P. 2014. Root  
694 cortical aerenchyma enhances nitrogen acquisition from low-nitrogen soils in  
695 maize. *Plant Physiol.* 166:726-735.
- 696 Senior, M., Chin, E., Lee, M., Smith, J., Stuber, C. 1996. Simple sequence repeat  
697 markers developed from maize sequences found in the GENBANK database: map  
698 construction. *Crop Sci.* 36:1676-1683.
- 699 Sexstone, A.J., Revsbech, N.P., Parkin, T.B., Tiedje, J.M. 1985. Direct  
700 measurement of oxygen profiles and denitrification rates in soil aggregates. *Soil  
701 Sci Soc Am J* 49:645-651.
- 702 Stahl, D.A., Torre, J.R.D.L. 2012. Physiology and diversity of ammonia-oxidizing  
703 archaea. *Annu. Rev. Microbiol.* 66:83-101.
- 704 Sterngren, A.E., Hallin, S., Bengtson, P. 2015. Archaeal ammonia oxidizers  
705 dominate in numbers, but bacteria drive gross nitrification in n-amended grassland  
706 soil. *Front Microbiol* 6: 1350.
- 707 Sul, W.J., Asuming-Brempong, S., Wang, Q., Turlousse, D.M., Penton, C.R.,  
708 Deng, Y., Rodrigues, J.L.M., Adiku, S.G.K., Jones, J.W., Zhou, J., Cole, J.R.,  
709 Tiedje, J.M. 2013. Tropical agricultural land management influences on soil  
710 microbial communities through its effect on soil organic carbon. *Soil Biol. Biochem.*  
711 65:33-38.
- 712 Van Deynze, A., Zamora, P., Delaux, P-M., Heitmann, C., Jayaraman, D.,  
713 Rajasekar, S., Graham, D., Maeda, J., Gibson, D., Schwartz, K.D., Berry, A.M.,

Page 35 of 48

714 Bhatnagar, S., Jospin, G., Darling, A., Jeannotte, R., Lopez, J., Weimer, B.C.,  
715 Eisen, J.A., Shapiro, H-Y., Ané, J-M., Bennett, A.B. 2018. Nitrogen fixation in a  
716 landrace of maize is supported by a mucilage-associated diazotrophic microbiota.  
717 PLoS Biol 16:e2006352.

718 Walters, W. A., Jin, Z., Youngblut, N., Wallace, J. G., Sutter, J., Zhang, W., et al.  
719 2018. Large-scale replicated field study of maize rhizosphere identifies heritable  
720 microbes. Proc. Natl. Acad. Sci. 115:7368–7373 Available at:  
721 <https://www.pnas.org/content/115/28/7368> [Accessed March 30, 2020].

722 York, L.M., Galindo-Castañeda, T., Schussler, J.R., Lynch, J.P. 2015. Evolution of  
723 US maize (*Zea mays* L.) root architectural and anatomical phenes over the past  
724 100 years corresponds to increased tolerance of nitrogen stress. J. Exp. Bot.  
725 66:2347-2358

726 York, L.M., Nord, E.A., Lynch, J.P. 2013. Integration of root phenes for soil  
727 resource acquisition. Front Plant Sci 4:355.

728 Zhao, M., Jones, C.M., Meijer, J., Lundquist, P-O., Fransson, P., Carlsson, G.,  
729 Hallin, S. 2017. Intercropping affects genetic potential for inorganic nitrogen cycling  
730 by root-associated microorganisms in *Medicago sativa* and *Dactylis glomerata*.  
731 Appl. Soil Ecol. 119:260-266.

732

Page 36 of 48

733 **TABLES**

734 Table 1. Permutational MANOVA results using weighted UniFrac as a distance  
735 metric for the experiments by site. The model for URBC (South Africa) was  
736 weighted UniFrac distance ~ Genotype\*Nitrogen\*RCA, and for RS (USA) the  
737 model was weighted UniFrac distance ~ Genotype\*RCA ; with Block as random  
738 effect (with the option strata of the function *adonis* of the package *vegan* in R). For  
739 RCA (root cortical aerenchyma), we used qualitative ranks (See Supplementary  
740 Table 3 to see the values of each rank and Fig. 4 for data distribution within ranks).  
741 Bulk soil samples were excluded.

742

743

| Site                | Factor                | SS     | % var explained | R <sup>2</sup> | P value |
|---------------------|-----------------------|--------|-----------------|----------------|---------|
| URBC (South Africa) | Genotype              | 0.2775 | 7.6             | 0.07598        | 0.839   |
|                     | Nitrogen              | 0.1218 | 3.3             | 0.03335        | 0.055   |
|                     | RCA                   | 0.3455 | 9.5             | 0.09459        | 0.401   |
|                     | Genotype:Nitrogen     | 0.2841 | 7.8             | 0.7778         | 0.785   |
|                     | Genotype:RCA          | 0.779  | 21.3            | 0.213          | 0.487   |
|                     | Nitrogen:RCA          | 0.295  | 8.1             | 0.0808         | 0.1     |
|                     | Genotype:Nitrogen:RCA | 0.091  | 2.5             | 0.0249         | 0.804   |
|                     | Residuals             | 1.458  | 39.9            |                |         |
|                     | Total                 | 3.6523 | 100.0           |                |         |
| RS (Pennsylvania)   | Genotype              | 0.477  | 30.042          | 0.30042        | 0.569   |
|                     | RCA                   | 0.105  | 6.593           | 0.06593        | 0.426   |
|                     | Genotype:RCA          | 0.646  | 40.705          | 0.40705        | 0.319   |
|                     | Residuals             | 0.359  | 22.660          |                |         |
|                     | Total                 | 1.586  | 100.000         |                |         |

744

Page 38 of 48

745 Table 2. Models of unweighted and weighted UniFrac distances as functions of  
 746 anatomical and architectural phenes at URBC (South Africa) and significance per  
 747 phene, as selected by random permutations. Constrained correspondence  
 748 analyses (CCA) were constrained by the factors Nitrogen, Genotype and Block.  
 749 percCisA: Percentage of cortex that is aerenchyma. TopAngle: Angle along the  
 750 outline of the root at 10% width accumulation. BottomAngle: Angle along the  
 751 outline of the root at 70% width accumulation. D10: Accumulated width over the  
 752 depth at 10% of the central path length.

| URBC unweighted UniFrac ANATOMY |  |      |         |
|---------------------------------|--|------|---------|
| Model:                          | distance= percCisA +Condition (Nitrogen+ Block)) |      |         |
| p value of the model            | 0.054  |      |         |
| Factor                          | SS   | F    | Pr (>F) |
| percCisA                        | 0.174  | 1.56 | 0.045   |
| Residual                        | 2.346  |      |         |
| URBC weighted UniFrac ANATOMY   |  |      |         |
| Model                           | distance = perCisA + Condition(Nitrogen + Block) |      |         |
| p value of the model            | 0.108  |      |         |

Page 39 of 48

| Factor                               | SS  | F      | Pr (>F) |
|--------------------------------------|---|--------|---------|
| percCisA                             | 0.0144  | 1.9768 | 0.092   |
| Residual                             | 0.153   |        |         |
| URBC unweighted UniFrac ARCHITECTURE |   |        |         |
| Model                                | distance = TopAngle + BottomAngle + D10 + Condition<br>(Nitrogen + Block) |        |         |
| p value of the<br>model              | 0.084   |        |         |
| Factor                               | SS  | F      | Pr (>F) |
| TopAngle                             | 0.522   | 0.927  | 0.522   |
| BottomAngle                          | 0.164   | 1.484  | 0.068   |
| D10                                  | 0.141   | 1.269  | 0.128   |
| Residual                             | 2.111   |        |         |
| URBC weighted UniFrac ARCHITECTURE   |   |        |         |
| Model                                | distance = TopAngle + BottomAngle + D10 Condition (Nitrogen<br>+ Block)   |        |         |
| p value of the<br>model              | 0.066   |        |         |

Page 40 of 48

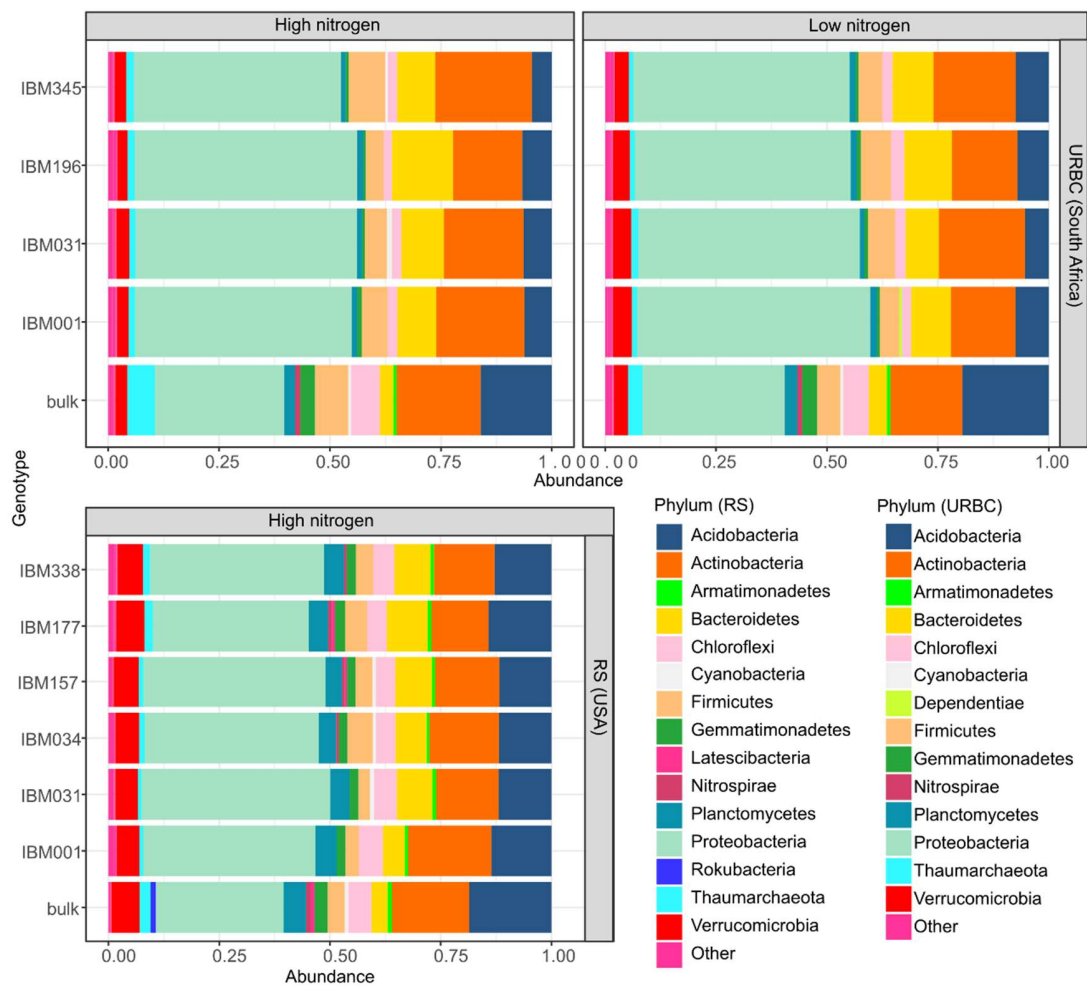
| Factor      | SS    | F    | Pr(>F) |
|-------------|-------|------|--------|
| TopAngle    | 0.009 | 1.28 | 0.244  |
| BottomAngle | 0.012 | 1.77 | 0.137  |
| D10         | 0.016 | 2.25 | 0.062  |
| Residual    | 0.131 |      |        |

753



754 **FIGURES**

755 Fig. 1. Bar plots of the relative abundances discriminating the 15 (for RS) and 14  
756 (for URBC) most abundant phyla in each rhizosphere sample and bulk soil by  
757 experimental site. Low abundance phyla are represented as “other”. Values are  
758 means of at least three replicates.

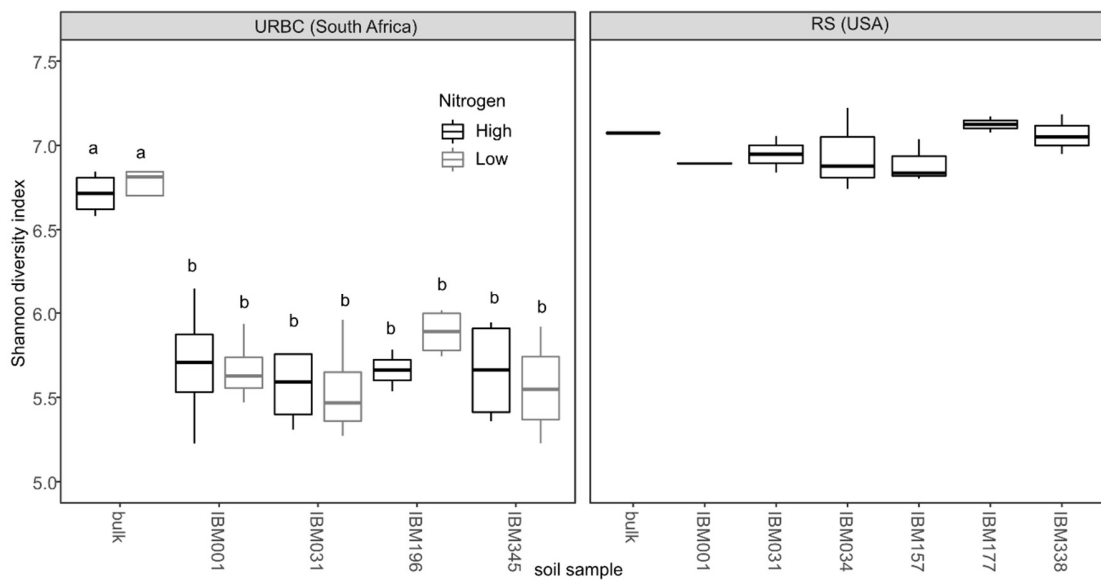


759

760

Page 42 of 48

761 Fig. 2. Alpha diversity of rhizosphere soil collected from all genotypes and bulk soil  
762 at the two sites. Horizontal box lines correspond to 25th, 50th, and 75th percentile;  
763 ranges are indicated by whiskers. For each boxplot  $n = 2-4$ . Boxes with the same  
764 letters indicate no significant differences in Shannon diversity indexes according  
765 to a LSD test with  $P < 0.05$ . No significant differences were found between  
766 genotypes (and bulk soil) at RS.

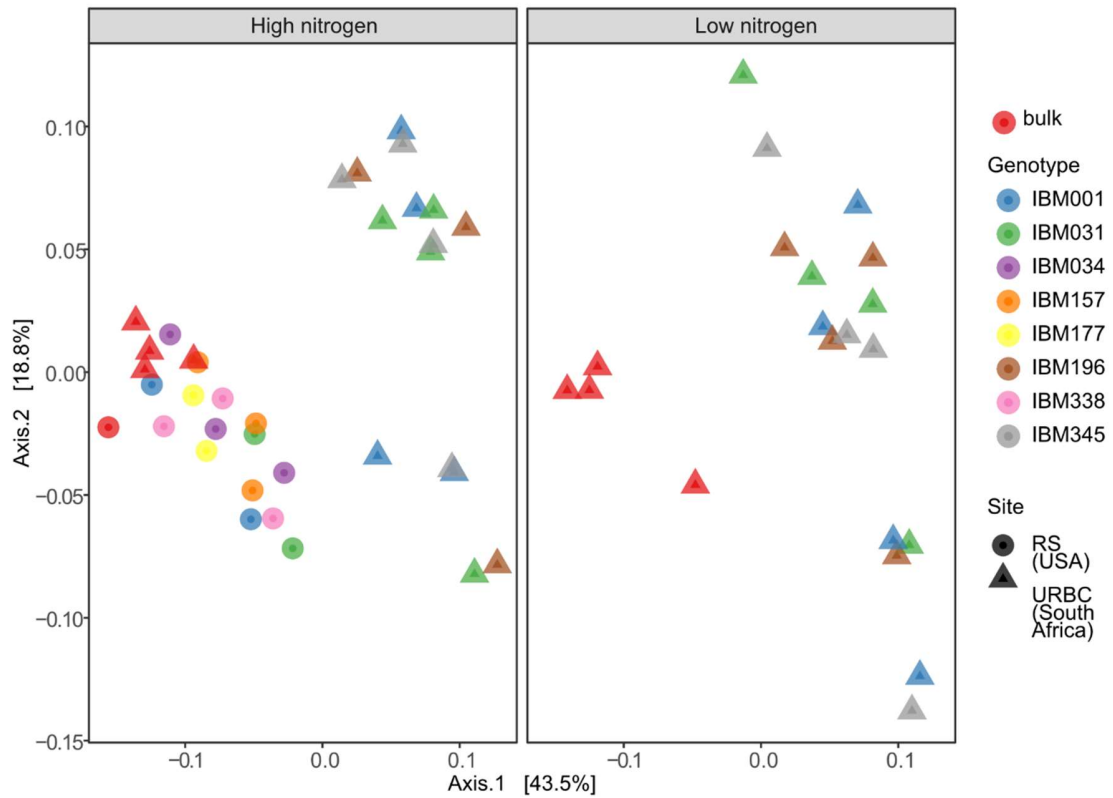


767

768

Page 43 of 48

769 Fig. 3. PCoAs using weighted UniFrac distances of the two sites, differentiated by  
770 genotypes. Nitrogen levels are in separate plots for URBC.

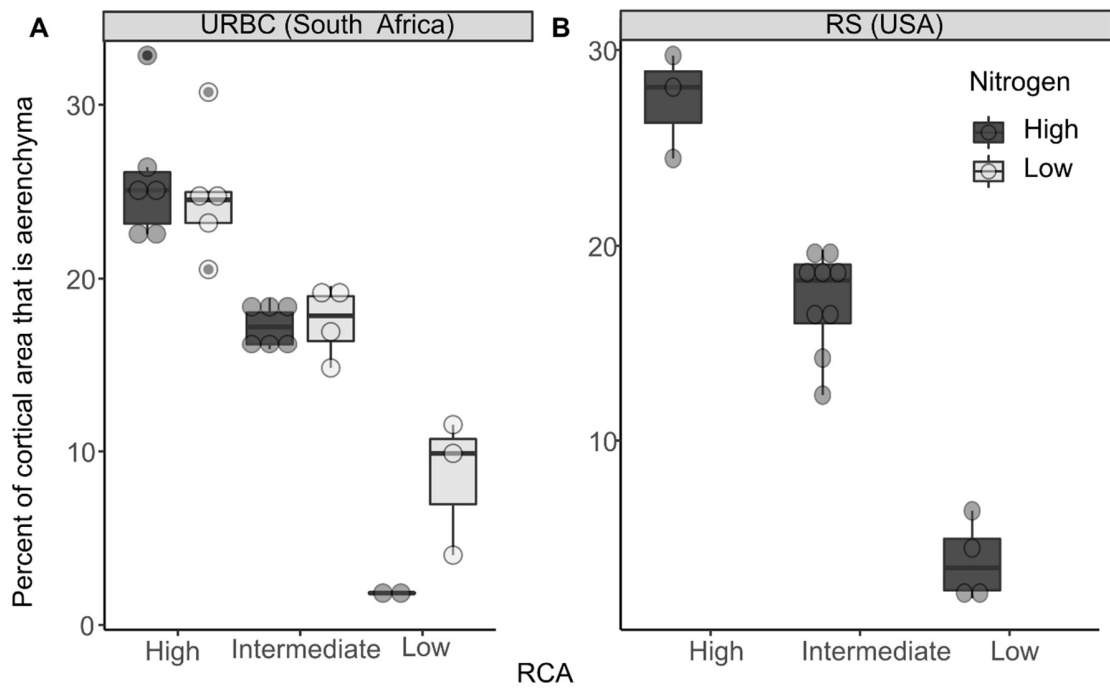


771

772

Page 44 of 48

773 Fig. 4. Bloxplots of percent cortical area that is aerenchyma (percCisA) by RCA  
774 ranks at the two sites. Horizontal box lines correspond to 25th, 50th, and 75th  
775 percentile; ranges are indicated by whiskers and points out of the boxes are  
776 outliers. For each boxplot the data points are indicated in open circles.

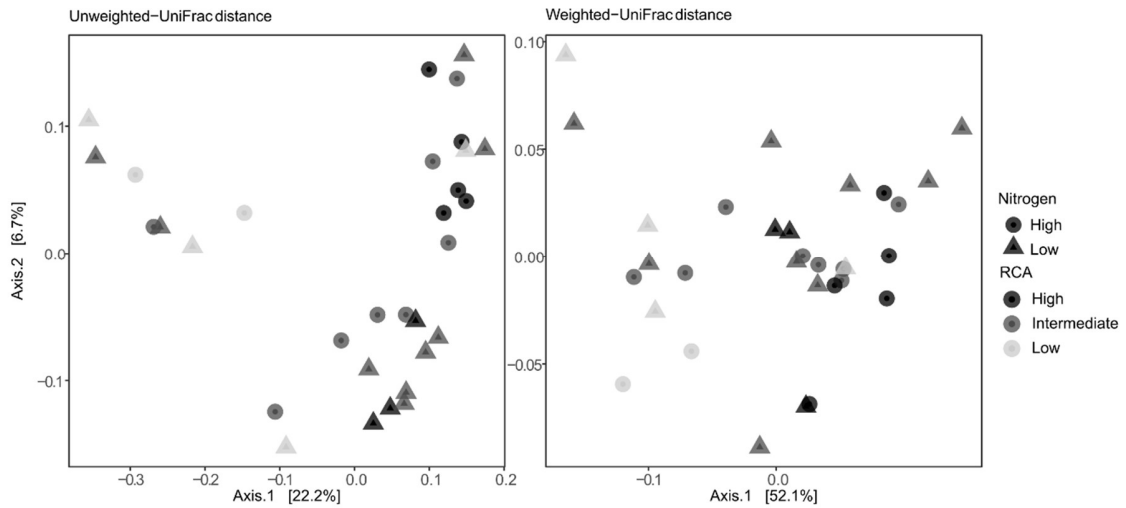


777

778

Page 45 of 48

779 Fig. 5. PCoAs using weighted and unweighted UniFrac distances by RCA  
780 qualitative ranks (determined as shown in Supplementary Table 3 and Fig.4), and  
781 additionally by nitrogen level at URBC.

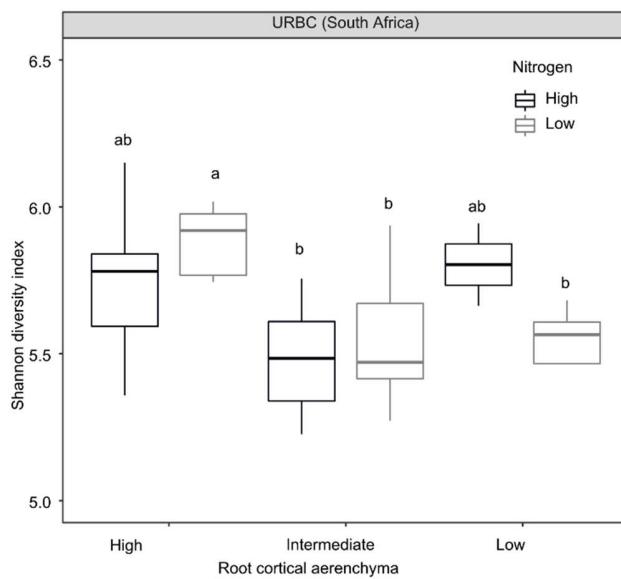


782

783

Page 46 of 48

784 Fig. 6. Boxplots of Shannon diversity values per RCA phenotype, and per nitrogen  
785 levels on rarefied data from URBC. Horizontal box lines correspond to 25th, 50th,  
786 and 75th percentile; ranges are indicated by whiskers. Letters indicate significant  
787 differences with a LSD test  $P < 0.05$ .



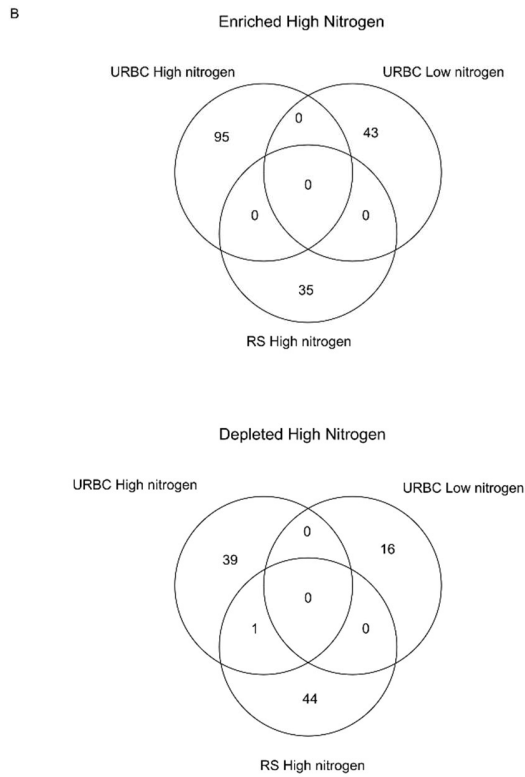
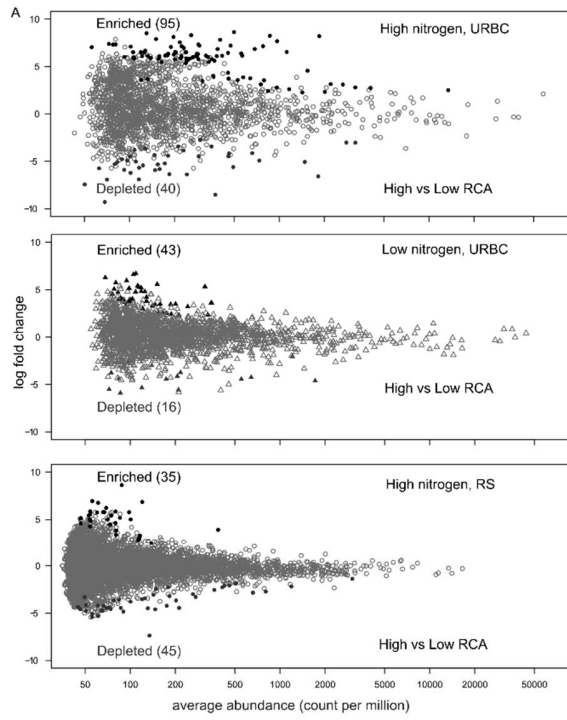
788

789

Page 47 of 48

790 Fig. 7. A: Abundance log change (y axis) of all the OTUs when RCA levels were  
791 compared within each RCA level. Black points indicate differentially enriched and  
792 depleted OTUs according to a likelihood ratio test with  $P < 0.01$ , and grey points  
793 were non-differentially abundant between the two types of samples, Number of  
794 OTUs significantly enriched or decreased at each condition are in parenthesis. B:  
795 Number of the differentially enriched and depleted OTUs between each RCA level  
796 and nitrogen level at the two sites.

Page 48 of 48





**Statement of author contributions:** J.P.L. and T.G.C. conceived and designed the research; T.G.C. conducted the experiments and performed statistical analysis; E.L.B. provided the facility to conduct the sequencing of DNA and provided technical and scientific assistance for the analysis and data interpretation; U.K. performed the UPARSE work of the raw sequences; C.R. performed the work with Qiime and provided technical assistance for the statistical analysis; T.G.C. and J.P.L. wrote the article with contributions of all the authors. J.P.L. agrees to serve as the author responsible for contact and ensures communication.

### Supplementary Tables

Supplementary Table 1. Summary of soil analyses performed at URBC (South Africa) and RS (USA) as an external service. Extraction methods: P - Bray I \ Olsen (pH  $\geq$  7.3), Cations – NH<sub>4</sub>OAc, Organic C - Walkley-Black method, Fe,Mn,Zn,Cu,Ni – DTPA, Tot-N - 0.1N K<sub>2</sub>SO<sub>4</sub>. NA: not available information.

| Measurement     | Units               | Values      |    |             |
|-----------------|---------------------|-------------|----|-------------|
|                 |                     | URBC        |    | RS          |
|                 |                     | LN          | HN | HN          |
| Bulk density    | g*cm <sup>3</sup>   | 1.250-1.511 |    | 1.400-1.600 |
| pH              | KCl                 | 3.8-5.3     |    | 6.7-7.3     |
| S               | mg*kg <sup>-1</sup> | 7.0 - 89.0  |    | 7.6-16.4    |
| P               | mg*kg <sup>-1</sup> | 16-73       |    | 35-111      |
| K               | mg*kg <sup>-1</sup> | 46-70       |    | 87-271      |
| Ca              | mg*kg <sup>-1</sup> | 86-240      |    | 1165-2907   |
| Mg              | mg*kg <sup>-1</sup> | 26-57       |    | 98-168      |
| ECEC            | Calculated          | 1.1-1.9     |    | 8.3-16.7    |
| Total N         | mg*kg <sup>-1</sup> | 6.0-13      | NA | NA          |
| NO <sub>3</sub> | mg*kg <sup>-1</sup> | 5.0-12      | NA | NA          |
| NH <sub>4</sub> | mg*kg <sup>-1</sup> | 1.0-3       | NA | NA          |
| Organic content | matter %            | 0.1-0.5     |    | 0.9-2       |

Supplementary Table 2. Permutational MANOVA results using weighted UniFrac as a distance metric for the experiments by site. The Adonis model for each experiment was: at URBC, weighted UniFrac distance ~ Soil type \* Nitrogen + Block, at RS weighted UniFrac distance ~ Soil type + Block. Soil type refers to rhizosphere soil and bulk soil.

| Site                | Factor             | SS    | % Explained | P value |
|---------------------|--------------------|-------|-------------|---------|
| URBC (South Africa) | Soil type          | 0.185 | 38.6        | 0.001   |
|                     | Nitrogen           | 0.010 | 2.1         | 0.224   |
|                     | Block              | 0.040 | 8.4         | 0.002   |
|                     | Soil type:Nitrogen | 0.005 | 1.0         | 0.58    |
|                     | Residuals          | 0.239 | 49.9        |         |
|                     | Total              | 0.479 |             |         |
| RS (USA)            | Soil type          | 0.012 | 11.4        | 0.001   |
|                     | Block              | 0.031 | 29.5        | 0.001   |
|                     | Residuals          | 0.063 | 60.0        |         |
|                     | Total              | 0.105 |             |         |

Supplementary Table 3. Values (in percentage) of RCA expressed as percent of the cortical area that is aerenchyma (percCisA) measured at RS and URBC.

| Site           | Phene states | Quantitative values |
|----------------|--------------|---------------------|
| URBC           | High         | >20                 |
| (South Africa) | Intermediate | 12 - 20             |
|                | Low          | <12                 |
| RS (USA)       | High         | >20                 |
|                | Intermediate | 10 - 20             |
|                | Low          | <10                 |

Supplementary Table 4. Descriptive statistics of anatomical and architectural phenes measured at URBC.

| Phene abbreviation | Description                             | Units           | Median   | Mean     | min      | max      | Variance | Standard Deviation | Coefficient of Variation |
|--------------------|---|-----------------|----------|----------|----------|----------|----------|--------------------|--------------------------|
| RXSA               | Root cross section area                 | mm <sup>2</sup> | 1.908    | 1.941    | 0.642    | 5.106    | 0.603    | 0.777              | 0.40                     |
| TCA                | Total cortex area                       | mm <sup>2</sup> | 1.423    | 1.426    | 0.454    | 3.657    | 0.310    | 0.557              | 0.39                     |
| TSA                | Total stele area                        | mm <sup>2</sup> | 0.495    | 0.537    | 0.172    | 1.644    | 0.066    | 0.257              | 0.48                     |
| AA                 | Aerenchyma area                         | mm <sup>2</sup> | 0.240    | 0.248    | 0.000    | 0.597    | 0.022    | 0.149              | 0.60                     |
| MXVA               | Total metaxylem vessel area             | mm <sup>2</sup> | 0.074    | 0.074    | 0.025    | 0.136    | 0.000    | 0.022              | 0.30                     |
| MXVS               | Mean metaxylem vessel size              | mm <sup>2</sup> | 0.006    | 0.006    | 0.002    | 0.013    | 0.000    | 0.002              | 0.26                     |
| MXVN               | Metaxylem vessel number                 | count           | 12.000   | 12.391   | 7.000    | 21.000   | 9.364    | 3.060              | 0.25                     |
| CCFN               | Cortical cell file number               | count           | 10.333   | 10.733   | 6.000    | 18.000   | 4.966    | 2.229              | 0.21                     |
| LCA                | Living cortical area                    | mm <sup>2</sup> | 0.221    | 0.263    | 0.107    | 1.093    | 0.028    | 0.168              | 0.64                     |
| CCS                | Cortical cell size                      | mm <sup>2</sup> | 0.000237 | 0.000259 | 0.000139 | 0.000456 | 0.000000 | 0.000082           | 0.315817                 |
| C:S                | Cortex:Stele ratio                      | dimensionless   | 2.673    | 2.805    | 1.661    | 4.928    | 0.431    | 0.656              | 0.23                     |
| perCisA            | Percentage of cortex that is aerenchyma | %               | 19.965   | 17.823   | 0.000    | 34.237   | 76.128   | 8.725              | 0.49                     |

|             |   |   |           |           |          |           |              |          |      |
|-------------|---|---|-----------|-----------|----------|-----------|--------------|----------|------|
| perCisCC    | Percentage of cortex that is LCA  | %   | 18.804    | 19.465    | 10.209   | 29.895    | 19.840       | 4.454    | 0.23 |
| perXSisCC   | Percentage of cross section that is LCA   | %   | 13.977    | 14.538    | 7.429    | 25.025    | 13.362       | 3.655    | 0.25 |
| S_Diam      | Stem diameter   | mm  | 14.852    | 14.376    | 6.988    | 18.771    | 6.020        | 2.454    | 0.17 |
| RootArea    | number of pixels that belong to the root system                                   | number of pixels                            | 16716.534 | 16598.836 | 7441.681 | 26802.388 | 21008886.169 | 4583.545 | 0.28 |
| RootDensity | Ratio between root and background pixels  | root pixels*background pixels <sup>-1</sup> | 3.696     | 3.879     | 1.262    | 7.287     | 1.747        | 1.322    | 0.34 |
| TopAngle    | Angle along the OTUline of the root at 10% width accumulation                     | Sexagesimal degree (°)                      | 7.289     | 22.820    | 0.061    | 68.237    | 583.971      | 24.165   | 1.06 |
| BottomAngle | Angle along the OTUline of the root at 70% width accumulation                     | Sexagesimal degree (°)                      | 26.228    | 25.418    | 0.552    | 44.612    | 134.372      | 11.592   | 0.46 |
| RootPaths   | Number of paths detected for the root system. Correlated with number of root tips | Count                                       | 542.000   | 594.031   | 249.000  | 1336.000  | 45409.843    | 213.096  | 0.36 |

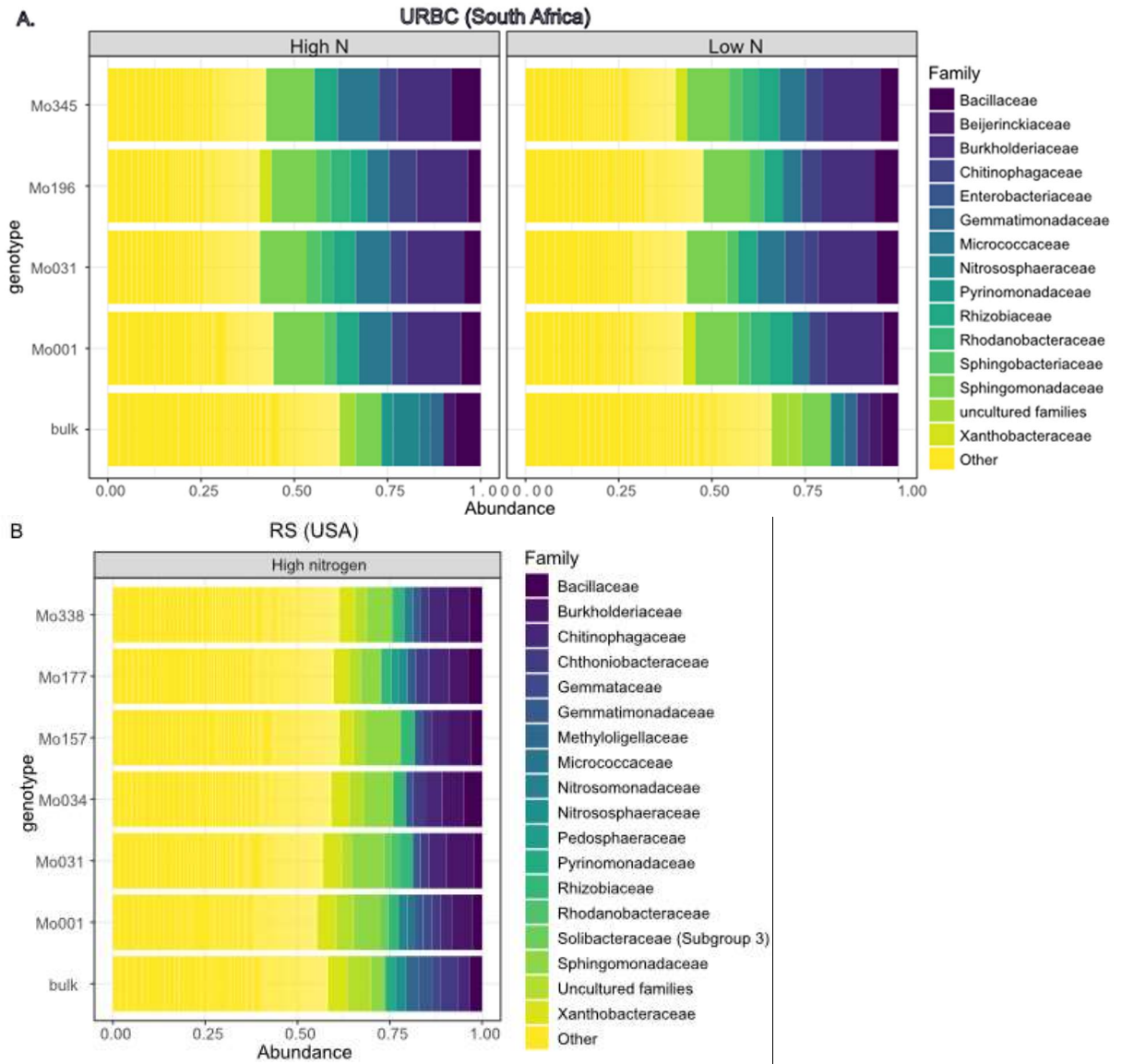
|                 |  |                                |         |         |         |         |          |        |      |
|-----------------|--|--------------------------------|---------|---------|---------|---------|----------|--------|------|
| D10             | Accumulated width over the depth at 10% of the central path length. Closely related to the root-top angle for maize. | %                              | 0.340   | 0.334   | 0.173   | 0.453   | 0.004    | 0.066  | 0.20 |
| LatRootLength   | Average length of the detected lateral roots emerging from the central path long of the excised roots                | cm                             | 193.399 | 192.664 | 137.866 | 268.145 | 1057.415 | 32.518 | 0.17 |
| NodalRootLength | Length of the central path along the excised root  | cm                             | 299.660 | 293.717 | 186.522 | 392.363 | 1999.905 | 44.720 | 0.15 |
| LatBD           | Lateral branching density  | lateral roots*cm <sup>-1</sup> | 11.985  | 12.436  | 1.293   | 31.368  | 56.974   | 7.548  | 0.61 |
| NodalRootDiam   | Average nodal root diameter  | µm                             | 174.402 | 170.041 | 13.120  | 294.623 | 3560.569 | 59.670 | 0.35 |
| DistFirstLat    | Distance to first lateral  | cm                             | 0.575   | 1.415   | 0.000   | 10.269  | 4.108    | 2.027  | 1.43 |

Supplementary Table 5. Descriptive statistics of anatomical phenes measured at RS.

| Phene abbreviation | Description                             | Units           | min    | max     | Median  | Mean    | Standard Error | Variance | Standard Deviation | Coefficient of Variation |
|--------------------|---|-----------------|--------|---------|---------|---------|----------------|----------|--------------------|--------------------------|
| RXSA               | Root cross section area                 | mm <sup>2</sup> | 0.576  | 2.750   | 1.229   | 1.261   | 0.096          | 0.222    | 0.472              | 0.37                     |
| TCA                | Total cortex area                       | mm <sup>2</sup> | 0.400  | 2.149   | 0.956   | 0.959   | 0.077          | 0.142    | 0.377              | 0.39                     |
| TSA                | Total stele area                        | mm <sup>2</sup> | 0.158  | 0.601   | 0.273   | 0.302   | 0.022          | 0.011    | 0.107              | 0.35                     |
| C:S                | Cortex:Stele ratio                      | dimensionless   | 1.816  | 4.951   | 3.316   | 3.200   | 0.142          | 0.481    | 0.693              | 0.22                     |
| AA                 | Aerenchyma area                         | mm <sup>2</sup> | 0.017  | 0.522   | 0.129   | 0.151   | 0.022          | 0.012    | 0.110              | 0.72                     |
| perCisA            | Percentage of cortex that is aerenchyma | %               | 1.930  | 29.710  | 16.498  | 15.645  | 1.562          | 58.559   | 7.652              | 0.49                     |
| MXVA               | Total metaxylem vessel area             | mm <sup>2</sup> | 0.034  | 0.136   | 0.059   | 0.066   | 0.005          | 0.001    | 0.025              | 0.37                     |
| MXVS               | Mean metaxylem vessel size              | mm <sup>2</sup> | 0.002  | 0.009   | 0.006   | 0.006   | 0.000          | 0.000    | 0.002              | 0.29                     |
| MXVN               | Metaxylem vessel number                 | count           | 8      | 20      | 10.5    | 11.639  | 0.773          | 14.347   | 3.788              | 0.33                     |
| CCFN               | Cortical cell file number               | count           | 7      | 13      | 9.5     | 9.597   | 0.279          | 1.865    | 1.365              | 0.14                     |
| LCA                | Living cortical area                    | mm <sup>2</sup> | 0.132  | 0.579   | 0.351   | 0.347   | 0.027          | 0.017    | 0.131              | 0.38                     |
| perCisCC           | Percentage of cortex that is LCA        | %               | 26.943 | 49.813  | 36.288  | 36.646  | 1.413          | 47.899   | 6.921              | 0.19                     |
| perXSisCC          | Percentage of cross section that is LCA | %               | 19.322 | 39.014  | 26.738  | 27.666  | 1.098          | 28.914   | 5.377              | 0.19                     |
| CCS                | Cortical cell size                      | mm <sup>2</sup> | 71.225 | 240.201 | 123.916 | 137.241 | 9.565          | 2195.808 | 46.859             | 0.34                     |

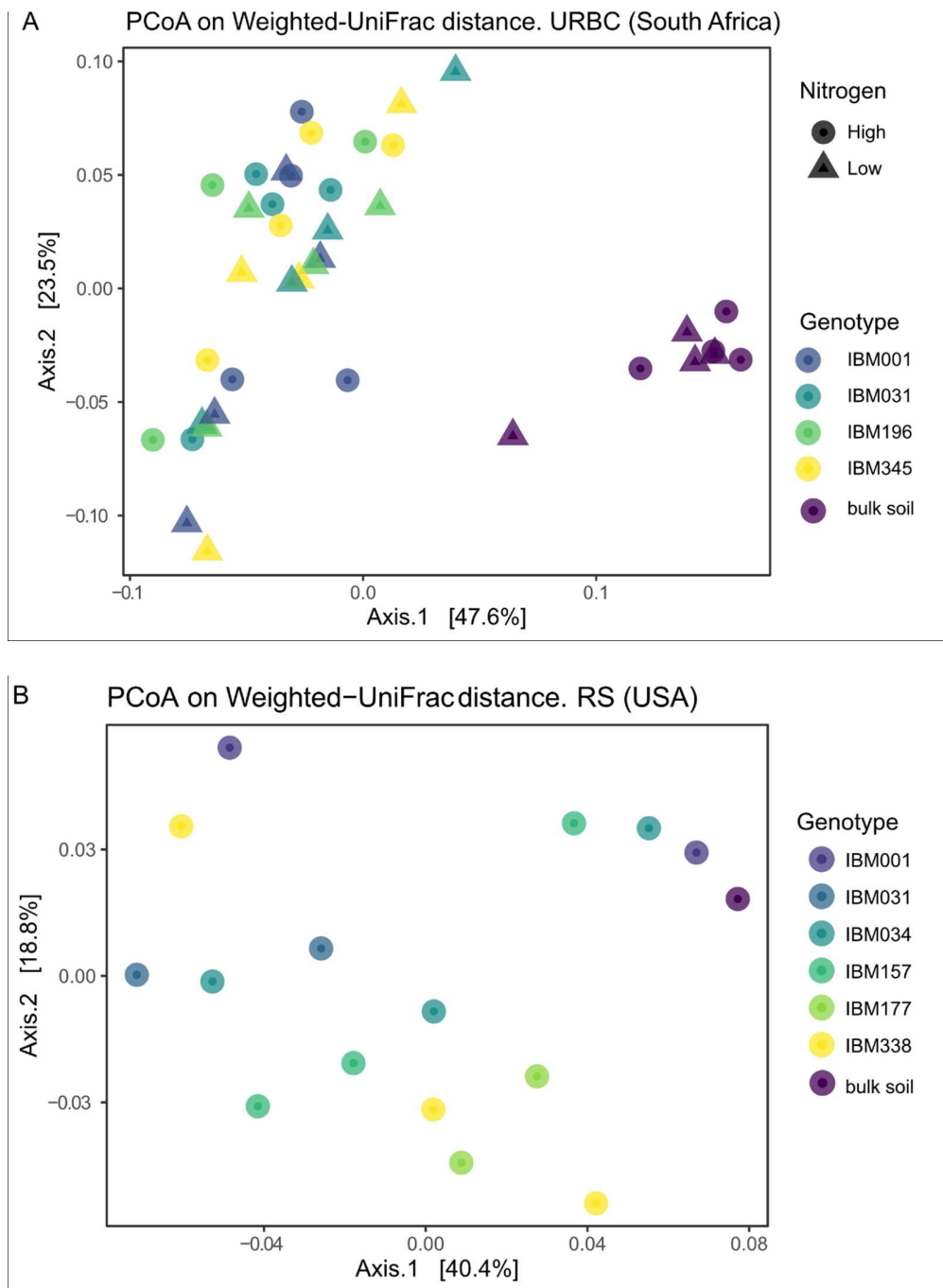
## Supplementary Figures





Supplementary Fig. 1. Bar plots of the relative abundances by family in each sample and experimental site. Families with abundances values below 0.03 (at URBC) and 0.02 (at RS) were grouped as “Other”. At RS (USA), uncultured families were distributed among 19 different phyla, among which *Actinobacteriaceae* and *Verrucomicrobia* were the most abundant. At URBC (South Africa), uncultured families were distributed among 14 phyla with *Actinobacteria* and *Acidobacteria* having the greatest abundance values.

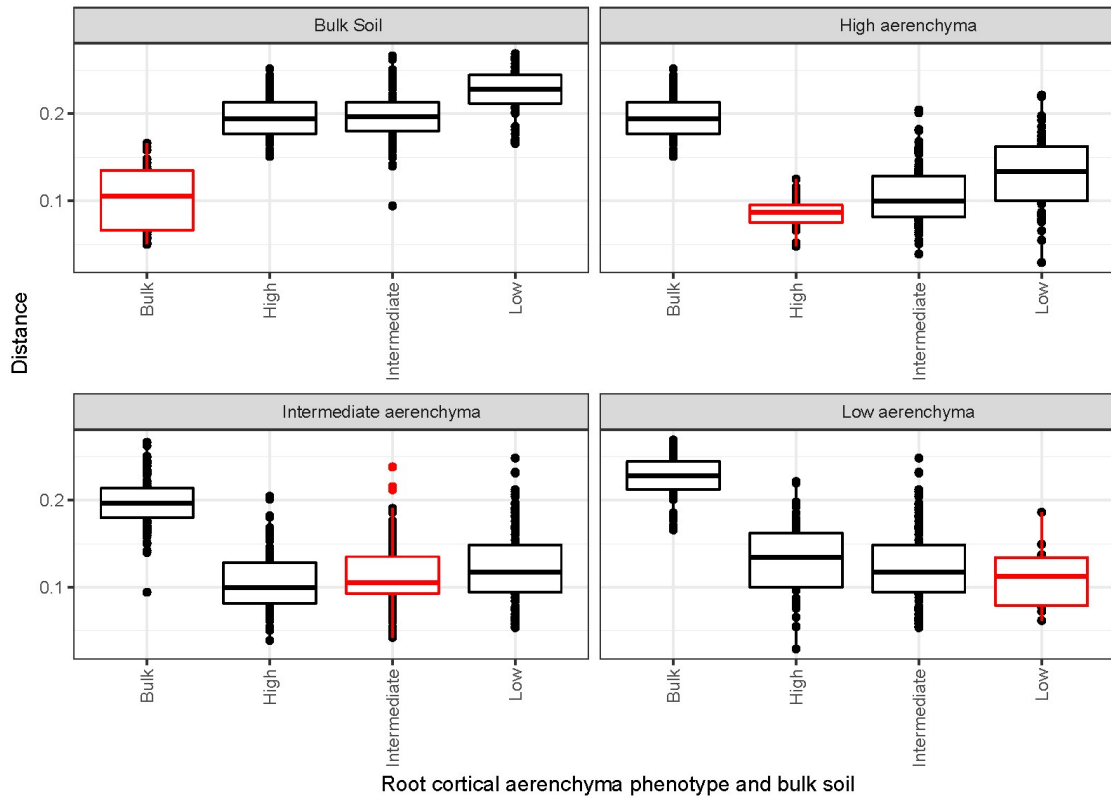
10



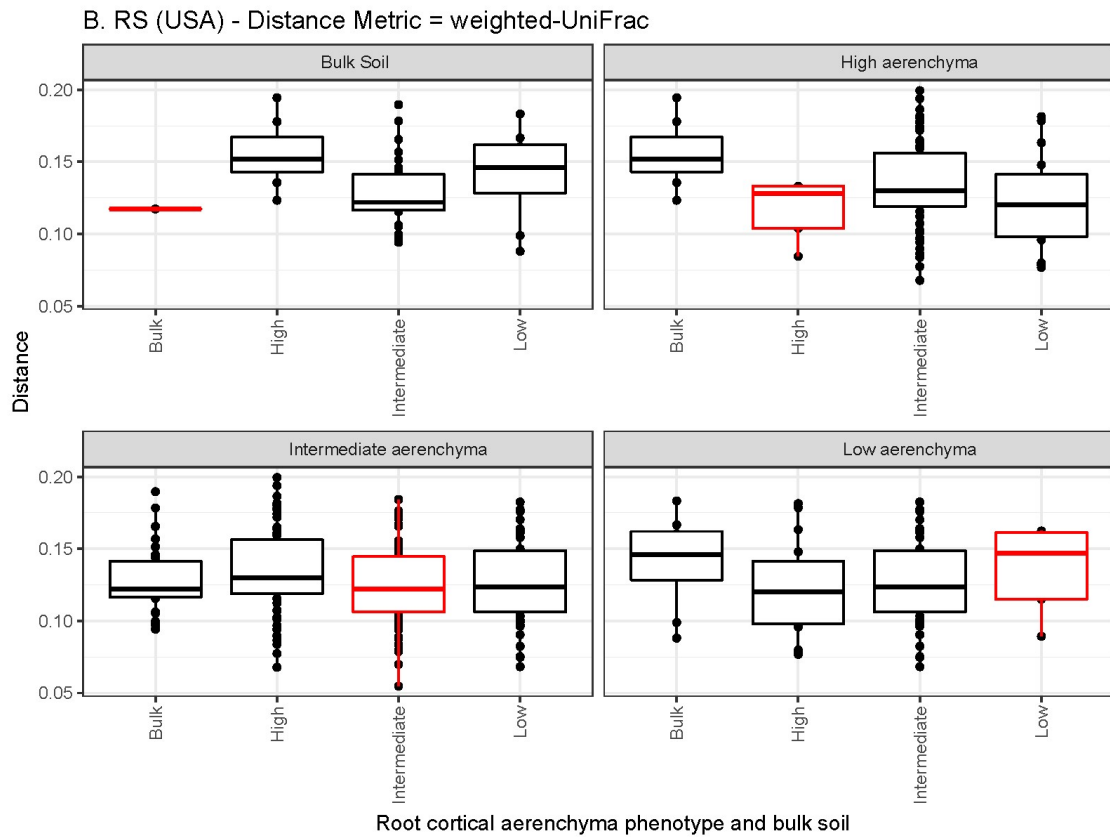
Supplementary Fig. 2. PCoAs using weighted UniFrac distances of each experimental site (A and B) by type of soil sample (rhizosphere vs bulk soil) in both sites, and additionally by nitrogen at URBC. Plots show the first two principal axes.

11

A. URBC (South Africa) - Distance Metric = weighted-UniFrac

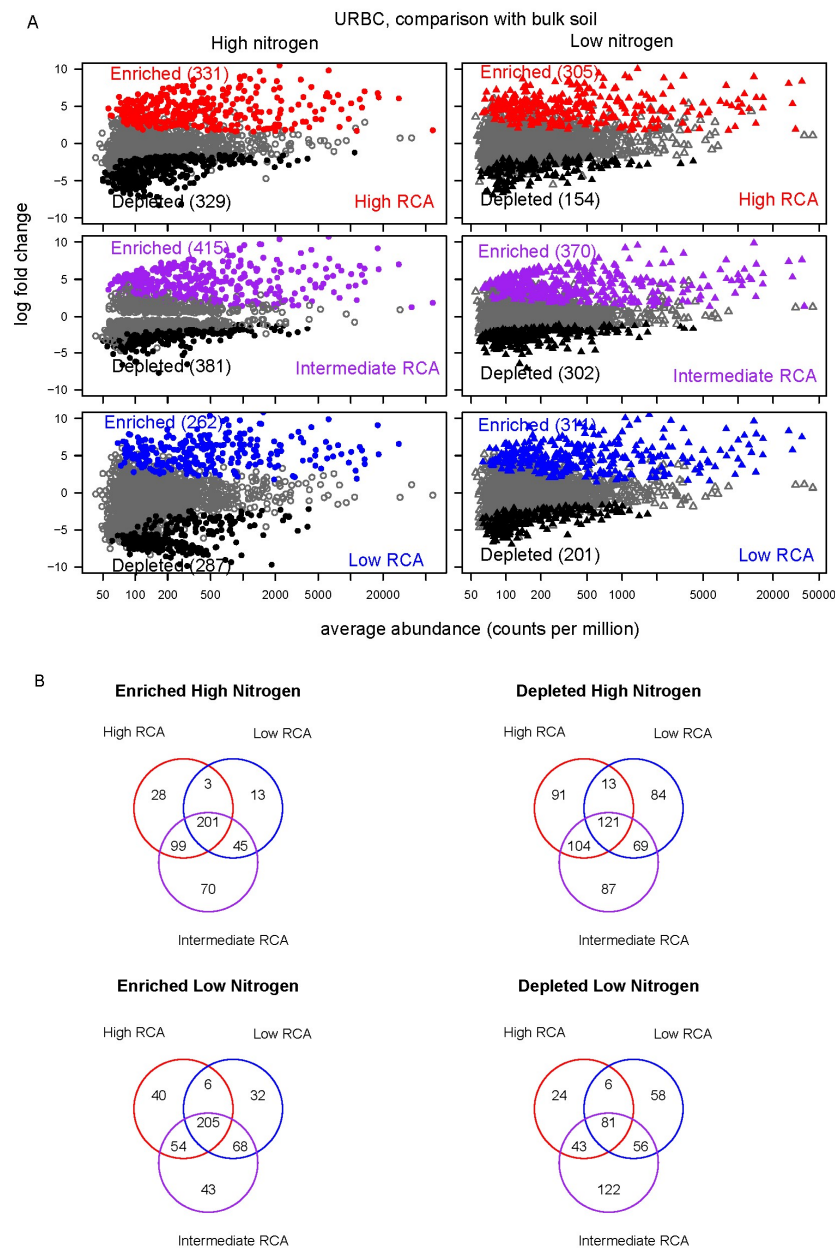


12



Supplementary Fig. 3. Boxplots comparing weighted-UniFrac distances between rhizosphere of plants of contrasting aerenchyma phenotype and bulk soil at URBC (A) and RS (B) on rarefied OTU counts. Horizontal box lines correspond to 25th, 50th, and 75th percentile; ranges are indicated by whiskers and points out of the boxes are outliers. Red-outlined boxplots correspond to self-comparison of the levels of phenotype or bulk soil.

13

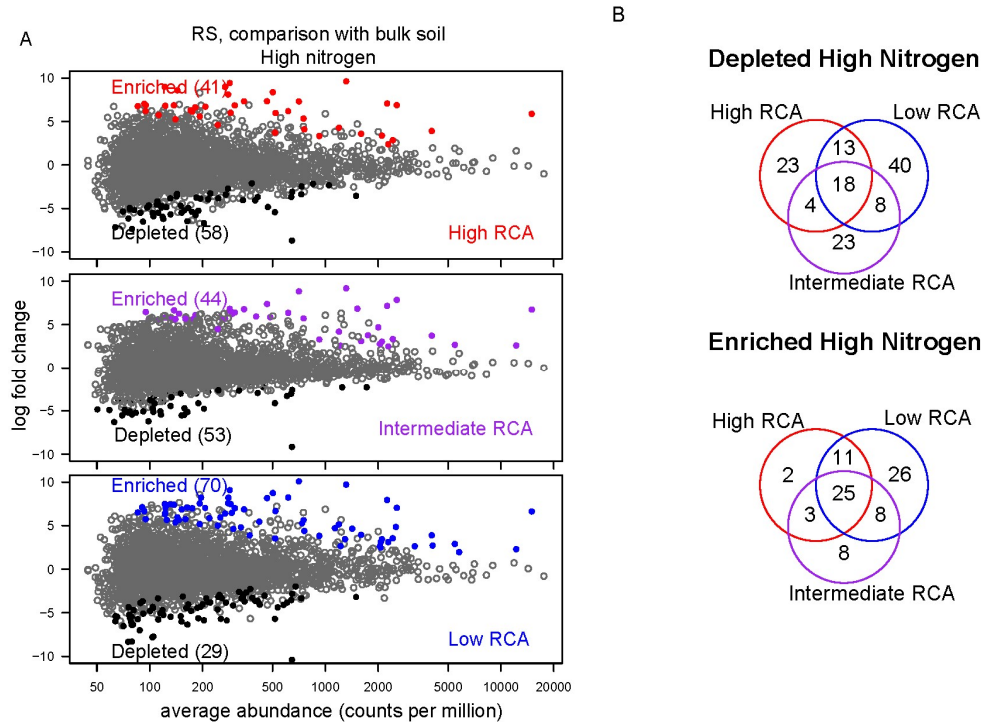


Supplementary Fig. 4. Abundance log change (y axis) of all the OTUs when rhizosphere (of each RCA rank) and bulk soil were compared at URBC (A). Colored points indicate differentially enriched (red, purple or blue) and depleted (black) OTUs according to a likelihood ratio test with  $P < 0.01$ , and grey points were non-differentially abundant between the respective rhizosphere and bulk soil samples. Number of OTUs significantly enriched or decreased at each condition

14

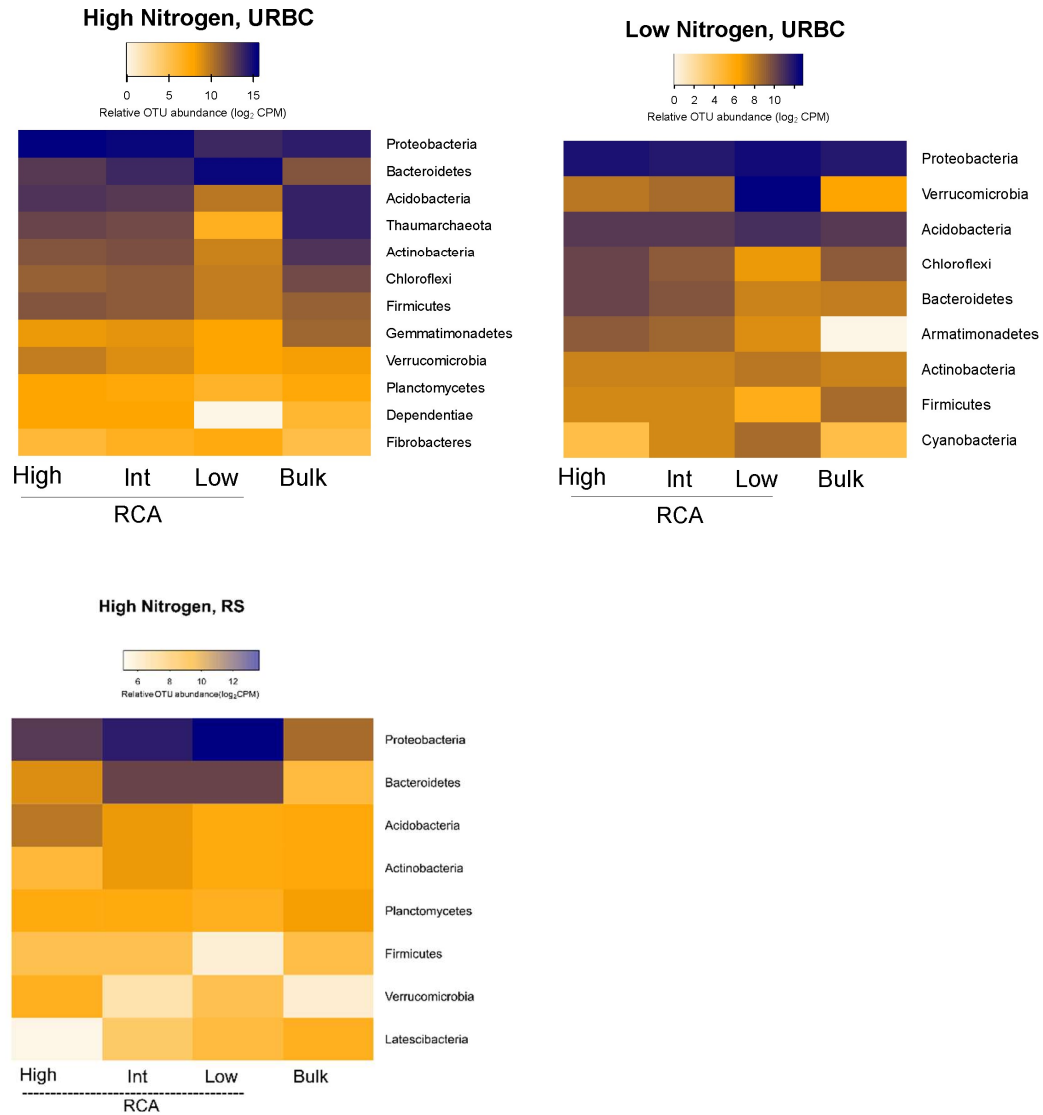
are in parenthesis. Number of the differentially enriched and depleted OTUs between each phenotype and bulk soil under the respective nitrogen level (B).

15



Supplementary Fig. 5. Abundance log change (y axis) of all the OTUs when rhizosphere (of each RCA rank) and bulk soil were compared at RS (A). Colored points indicate differentially enriched (red, purple or blue) and depleted (black) OTUs according to a likelihood ratio test with  $p < 0.01$ , and grey points were non-differentially abundant between the respective rhizosphere and bulk soil samples. Number of OTUs significantly enriched or decreased at each condition are in parenthesis. Number of the differentially enriched and depleted OTUs between each phenotype and bulk soil under the respective nitrogen level (B).

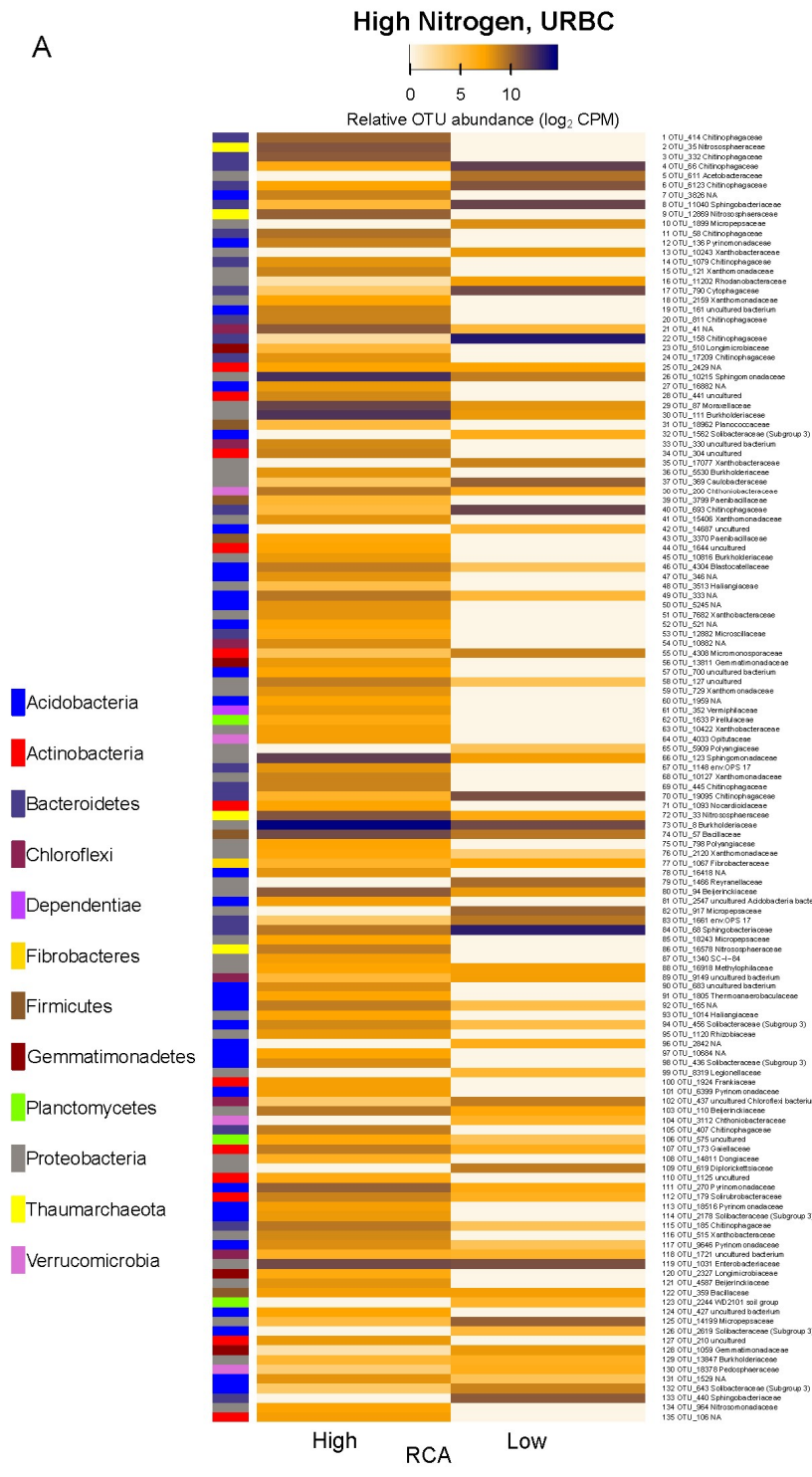
16



Supplementary Fig. 6. Mean relative abundances (counts per million, CPM; log<sub>2</sub> scale) of RCA-sensitive OTUs (found as described in Fig. 6), summarized at phylum level under high and low nitrogen at URBC and under high nitrogen at RS and in comparison with the abundance values of bulk soil.



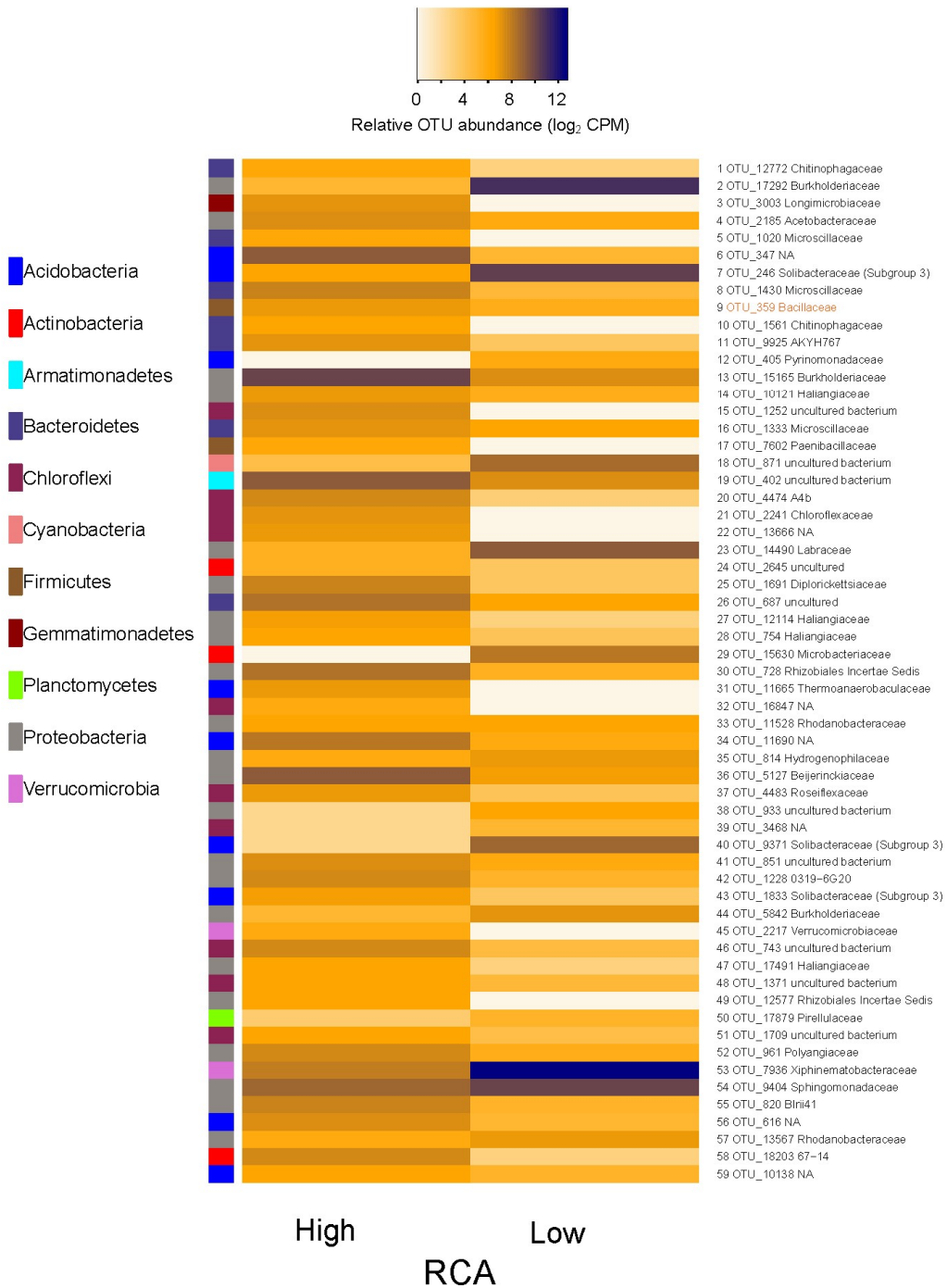
17



18

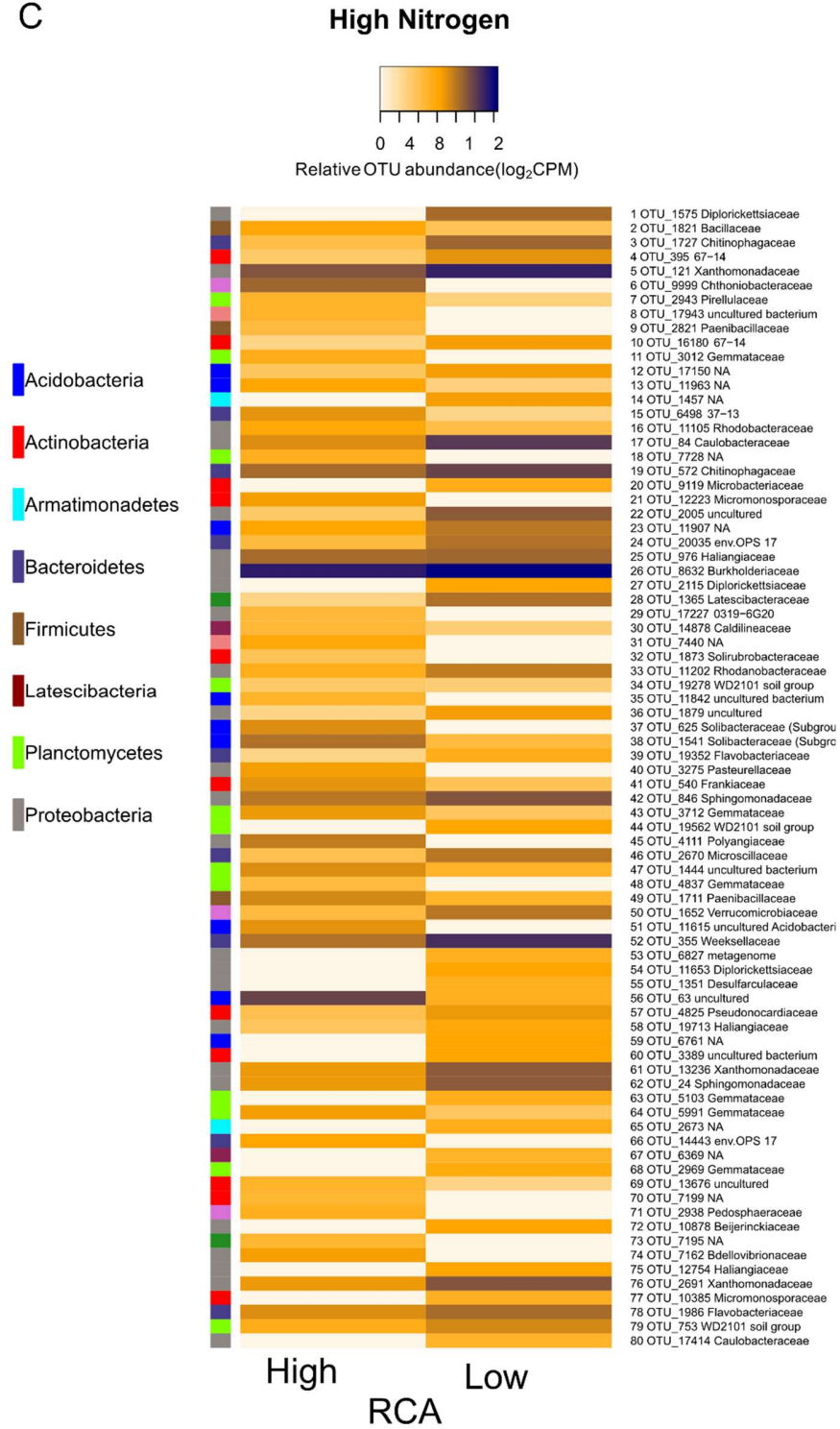
**B**

**Low Nitrogen, URBC**



19

C



20

Supplementary Fig. 7. Mean relative abundances (counts per million, CPM; log<sub>2</sub> scale) of RCA-sensitive OTUs (found as described in Fig. 6) at URBC (A,B) and at RS (C), summarized at family level (listed on right). Lists of the families and genera are also provided in File S1. The phyla are given in the colored bar of each graph (on left).

## Supplementary Results

### **Taxonomy and putative functions of enriched OTUs at contrasting RCA phenotypes**

Among the most abundant OTUs of high-RCA in high nitrogen conditions at URBC (South Africa), the families Comamonadaceae and Xanthomonadaceae and the genus *Sphingomonadaceae* (formerly classified as *Kaistobacter*, family Sphingomonadaceae) have been associated with disease-suppressive soils (Li et al., 2015; Liu et al., 2016). Bacteria of the nitrogen fixing families Beijerinckiaceae, Frankiaceae, and Rhizobiaceae were significantly enriched in high-RCA rhizospheres under high nitrogen, as well as ammonia oxidizing archaeans of the family Nitrososphaeraceae, and nitrate-reducers Gaiellaceae, Solirubrobacteraceae in addition to members of the phylum Acidobacteria and Actinobacteria that have been associated with the reduction of nitrate to nitrite by the assimilatory pathway (Albuquerque and da Costa, 2014a; Albuquerque and da Costa, 2014b; Campbell, 2014). Also, the family Chitinophagaceae which can degrade different organic macromolecules such as chitin and cellulose (McBride et al., 2014; Rosenberg, 2014), were found abundant in high-RCA plants under high nitrogen. At URBC, Low-RCA plants growing under high nitrogen conditions had three times less enriched OTUs compared to high-RCA. The two most abundant families among the enriched OTUs in low-RCA plants and high nitrogen were Sphingobacteriaceae and Chitinophagaceae (both from the phylum Bacteroidetes). Sphingobacteriaceae are aerobes chemoorganotrophs (Lambiase, 2014), and Chitinophagaceae are aerobes or facultative anaerobes with the potential to degrade macromolecules such as proteins, lipids, starch, pectin, chitin, carboxymethylcellulose or cellulose (McBride et al., 2014; Rosenberg, 2014).

Rhizospheres from low nitrogen plots at URBC had overall lower OTU abundances and a similar enriched-OTU distribution among the most abundant phyla compared to high nitrogen, with the difference that Armatimonadetes, a family generally considered aerobic of oligotrophic metabolism (Lee et al., 2014) was uniquely enriched under low nitrogen in high and intermediate RCA plants, and Cyanobacteria was enriched in low-RCA plants (Supplementary Fig. 7). Another difference between the high and low nitrogen treatments at URBC was the lack of enrichment of the family Nitrososphaeraceae of high-RCA plants under low nitrogen. Similarly to the high nitrogen treatment, bacteria of the family Burkholderiaceae were enriched in high-RCA rhizospheres at low nitrogen, as well as nitrogen-fixing symbionts such as Rhizobiales and Beijerinckiaceae (Genus *Microvirga*, File S1), and the family Sphingomonadaceae from the phylum Proteobacteria that have been reported in soil and rhizosphere microbial surveys (Castillo et al., 2017; Lebeis et al., 2015; Schmid et al., 2017; Vik et al., 2013).

Among the OTUs with the highest abundance at high-RCA in high nitrogen at RS (USA), we found the genus *Oceanobacillus* (Phylum Firmicutes), previously reported in rhizosphere of halophyte plant species as betaine and proline producer and phosphate solubilizer (Mukhtar et al. 2018; El-Tarabily and Youssef, 2010). The most abundant OTUs enriched at low-RCA belonged to the familie Diplorickettsiaceae of the phyllym Proteobacteria (Genus *Aquicella*), a pathogen to protozoans (Albuquerque et al., 2018), and Chitinophagaceae of the phylum Bacteroidetes (genus *Chitinophaga*) common inhabitant of maize rhizospheres (Walters et al., 2018).

### Literature cited in Supplementary Results

Albuquerque L, Da Costa MS (2014a) The Families Conexibacteraceae, Patulibacteraceae and Solirubrobacteraceae. *In*: Rosenberg E, Delong EF, Lory S, Stackebrandt E, Thompson F (eds.) *The Prokaryotes: Actinobacteria*. Berlin, Heidelberg: Springer Berlin Heidelberg.

Albuquerque L, Da Costa MS (2014b) The Family Gaiellaceae. *In*: Rosenberg E, Delong EF, Lory S, Stackebrandt E, Thompson F (eds.) *The Prokaryotes: Actinobacteria*. Berlin, Heidelberg: Springer Berlin Heidelberg.

Albuquerque, L., Rainey, F. A., and da Costa, M. S. 2018. Aquicella. In Bergey's Manual of Systematics of Archaea and Bacteria, Chichester, UK: John Wiley & Sons, Ltd, p. 1–9. Available at: <http://doi.wiley.com/10.1002/9781118960608.gbm01465> [Accessed March 31, 2020].

Campbell BJ (2014) The Family Acidobacteriaceae. *In*: Rosenberg E, Delong EF, Lory S, Stackebrandt E, Thompson F (eds.) *The Prokaryotes: Other Major Lineages of Bacteria and The Archaea*. Berlin, Heidelberg: Springer Berlin Heidelberg.

Castillo JD, Vivanco JM, Manter DK (2017) Bacterial Microbiome and Nematode Occurrence in Different Potato Agricultural Soils. *Microb Ecol* 74: 888-900

El-Tarabily, K. A., and Youssef, T. 2010. Enhancement of morphological, anatomical and physiological characteristics of seedlings of the mangrove *Avicennia marina* inoculated with a native phosphate-solubilizing isolate of *Oceanobacillus picturae* under greenhouse conditions. *Plant Soil*. 332:147–162.

Lebeis SL, Paredes SH, Lundberg DS, Breakfield N, Gehring J, Mcdonald M, Malfatti S, Glavina Del Rio T, Jones CD, Tringe SG, Dangl JL (2015) Salicylic acid modulates colonization of the root microbiome by specific bacterial taxa. *Science* 349: 860-864

Lee KCY, Dunfield PF, Stott MB (2014) The Phylum Armatimonadetes. *In*: Rosenberg E, DeLong EF, Lory S, Stackebrandt E, Thompson F (eds.) *The Prokaryotes: Other Major Lineages of Bacteria and The Archaea*. Berlin, Heidelberg: Springer Berlin Heidelberg.

Li X, Zhang YN, Ding C, Jia Z, He Z, Zhang T, Wang X (2015) Declined soil suppressiveness to *Fusarium oxysporum* by rhizosphere microflora of cotton in soil sickness. *Biol Fertility Soils* 51: 935-946

Liu X, Zhang S, Jiang Q, Bai Y, Shen G, Li S, Ding W (2016) Using community analysis to explore bacterial indicators for disease suppression of tobacco bacterial wilt. *Scientific reports* [Online] 6:

Mcbride MJ, Liu W, Lu X, Zhu Y, Zhang W (2014) The Family Cytophagaceae. *In*: Rosenberg E, DeLong EF, Lory S, Stackebrandt E, Thompson F (eds.) *The Prokaryotes: Other Major Lineages of Bacteria and The Archaea*. Berlin, Heidelberg: Springer Berlin Heidelberg.

Mukhtar, S., Mehnaz, S., Mirza, M. S., Mirza, B. S., and Malik, K. A. 2018. Diversity of *Bacillus*-like bacterial community in the rhizospheric and non-rhizospheric soil of halophytes (*Salsola stocksii* and *Atriplex amnicola*), and characterization of osmoregulatory genes in halophilic *Bacilli*. *Can. J. Microbiol.* 64:567–579.

Rosenberg E (2014) The Family Chitinophagaceae. *In*: Rosenberg E, DeLong EF, Lory S, Stackebrandt E, Thompson F (eds.) *The Prokaryotes: Other Major Lineages of Bacteria and The Archaea*. Berlin, Heidelberg: Springer Berlin Heidelberg.

Schmid CaO, Schröder P, Armbruster M, Schloter M (2017) Organic Amendments in a Long-term Field Trial—Consequences for the Bulk Soil Bacterial Community as Revealed by Network Analysis. *Microb Ecol*

Vik U, Logares R, Blaaid R, Halvorsen R, Carlsen T, Bakke I, Kolstø A-B, Økstad OA, Kauserud H (2013) Different bacterial communities in ectomycorrhizae and surrounding soil. *Scientific Reports* 3: 3471

Walters, W. A., Jin, Z., Youngblut, N., Wallace, J. G., Sutter, J., Zhang, W., et al. 2018. Large-scale replicated field study of maize rhizosphere identifies heritable microbes. *Proc. Natl. Acad. Sci.* 115:7368–7373 Available at: <https://www.pnas.org/content/115/28/7368> [Accessed March 30, 2020].